872

UNIVERSITE DE NEUCHATEL - INSTITUT DE PHYSIQUE

ETUDES OPTIQUES ET MAGNETO-OPTIQUES DE CRISTAUX D'IODURE DE CESIUM DOPES AU SODIUM

forme réduite de la

THESE

présentée à la Faculté des Sciences
de l'Université de Neuchâtel
pour l'obtention du grade de docteur ès sciences

par

A.-H. Kayal

Ingénieur-physicien diplômé EPFL

mai 1981

IMPRIMATUR POUR LA THÈSE

Etudes optiques et magnéto-optiques de cristaux d'iodure de Césium dopés au Sodium

de M onsieur Abdul-Hamid Kayal

UNIVERSITÉ DE NEUCHATEL

FACULTÉ DES SCIENCES

La Faculté des sciences de l'Université de Neuchâtel, sur le rapport des membres du jury,

Messieurs J. Rossel, C. Jaccard, A.M. Stoneham (Harwell) et Y. Mori (Osaka)

autorise l'impression de la présente thèse.

Neuchâtel, le 29 mars 1982

Le doyen:

A. Aeschlimann

phys. stat. sol. (b) **110**, 115 (1982)

Subject classification: 13.5.1 and 20.3; 19; 22.5.2

Institute of Physics, University of Neuchâtel[1])

Excitons Perturbed by a Sodium Ion in CsI:Na Crystal

By

A.-H. KAYAL, Y. MORI[2]), and J. ROSSEL

The emissions around 420 and 370 nm of CsI:Na excited by the UV absorption associated with the Na^+ ion are studied by measuring the temperature dependence of decay times, the magnetic circular polarization, and ESR by optical detection. The results suggest that the 420 nm band is due to a localized exciton adjacent to a substitutional Na^+ ion. The basic properties of the electronic structure and kinetics of the exciton are obtained. These results are discussed in relation with the self-trapped excitons in CsI.

Les émissions à 420 et 370 nm, du CsI:Na excité dans la région d'absorption UV associée a l'ion Na^+, sont étudiées en mesurant l'évolution des temps de déclin en fonction de la température, la polarisation magnétique circulaire et la RPE par detection optique. Les résultats suggèrent que la bande à 420 nm est due à un exciton localisé sur un ion Na^+ en position substitutionnelle. Les proprietés fondamentales de la structure électronique et la cinétique de l'exciton sont déterminées. Les résultats sont discutés en relation avec l'exciton autopiégé dans le CsI.

1. Introduction

In CsI crystals, the 338 and 290 nm emission bands of the self-trapped excitons (STE) have been studied experimentally [1 to 3] and a model describing their ionic and electronic structures has been proposed [4, 5]. In CsI crystals doped with NaI, two additional emissions peaking around 420 and 370 nm (called here 420 and 370 bands) occur under UV excitation [6, 7] just below the first excitonic absorption band. This very efficient 420 nm emission occurs also under ionizing irradiation [7] and even after such irradiation at low temperature [8, 9].

In the previous paper [7], the absorption, excitation, and emission spectra associated with Na^+ ions in CsI:Na were investigated with both UV and X-ray excitation for $4.2\,\mathrm{K} < T < 300\,\mathrm{K}$ and for different doping rates of Na^+. The study of emitting centers was done by measuring the temperature dependence of the decay times of 420 and 370 bands. Each of the former and the latter emissions was attributed to a single sort of exciton which is composed of singlet + triplet states and triplet state, respectively.

In the present work, further experiments on those emissions in CsI:Na, especially the measurement of the magnetic circular polarization (MCP) and the electron spin resonance (ESR), have been carried out under UV excitation. The analysis of the experimental results gives the nature of the electronic structure of the localized excitons and leads to the proposal that the 420 band is due to an exciton localized at a substitutional Na^+ ion.

Experimental procedures and results of absorption, excitation, and emission spectra,

[1]) Breguet 1, CH-2000 Neuchâtel, Switzerland.

[2]) Present address: Department of Applied Physics, Osaka City University, Sumiyoshi-ku, Osaka, Japan 558.

decay times, ESR and MCP will be shown in Sections 2 and 3, respectively. The nature of the excitons will be obtained in Section 5 by the analysis of the results based on the model introduced in Section 4. The proposed model of an exciton localized at a Na^+ ion will be obtained by discussing this nature in Section 6. Conclusion will be given in Section 7.

2. Experimental Procedures

Single crystals of CsI doped with NaI (10 to 1500 ppm) were grown in our laboratory by the Czochralski method from Merck suprapure powder. The samples, cut generally with (100) faces in suitable sizes, were polished and annealed at 450 °C to eliminate internal strains. They were mounted in a He-flow-type cryostat for the optical measurements or in a variable temperature cryostat with a split-coil superconducting magnet for the magneto-optical measurements.

For the measurement of the emission and the excitation spectra in the temperature region $4.2\ \mathrm{K} < T < 300\ \mathrm{K}$, we used a conventional arrangement. The light from a deuterium lamp goes to the sample through a prism monochromator "Leitz". The emission was detected at right angles by an "EMI 9558QB" photomultiplier tube (PM) through a second prism monochromator. For the decay time measurements, the deuterium lamp was replaced by a home-made nanosecond pulse discharge deuterium lamp [10]. The detection system was composed of a cooled PM "RCA C31000 M" followed by a time-resolved single-photon counting system. This system consists basically of a time to pulse-height converter (TAC) "Ortec 437" and a multichannel pulse-height analyser "NS 575A, Northern". With this statistical sampling method, we were able to measure decay-time constants between 1 ns and 100 μs.

For magneto-optical measurements, the magnetic field ($\boldsymbol{H}_0$) was applied parallel to a ⟨100⟩ crystal axis and the emission was detected along the same direction as $\boldsymbol{H}_0$. Adopting a conventional set-up with a stress birefringent modulator, we measured the MCP of the emissions under UV excitation for $T > 1.4$ K.

Optical detection of ESR was performed by replacing the optical tail in the experiment above by either X or Q band microwave cavities; each of them has two holes for the excitation and the detection. The microwave systems have microwave switches for the power modulation at 700 Hz. The emission intensity of either 370 band or 420 band has been detected synchronously with the modulation frequency of the microwave power. Detailed descriptions of all of these experimental procedures are given in [10].

3. Experimental Results

3.1 Absorption and excitation

CsI:Na shows an UV absorption peaking at 230 nm which is just below the first excitonic absorption band in CsI at 4.2 K [7]. It shifts to the lower-energy side when the temperature increases. Excitation in this UV region leads to the emission of 420 and 370 bands. The latter one has an efficiency of a few per cent of the former.

3.2 Emission spectra

Fig. 1b shows the emission spectrum of CsI:Na when it is excited at a favorable wavelength (238 nm) for the 370 band. The peak position and half-width ΔE of both bands are temperature dependent [7]; their values are, respectively, (368 ± 2) nm and $(0.27 \pm \pm 0.03)$ eV for the 370 band at 4.2 K in CsI:Na. Under continuous excitation, the intensity of the 420 band remains nearly constant in the temperature region between 1.4 and 300 K, while that of the 370 band decreases by increasing the temperature and disappears around 250 K.

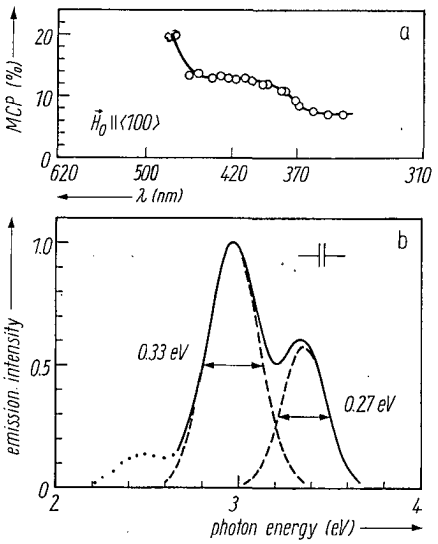

Fig. 1. a) Emission wavelength dependence of the MCP at $H_0 = 51$ kG and $T = 2$ K; b) emission spectrum of CsI:Na at 5 K under the UV excitation at 238 nm. The experimental result (solid line) is decomposed into two symmetric Gaussians (dashed lines)

3.3 Temperature dependence of the decay times

The emission decay of the 420 band after UV pulse excitation at 44 K is composed of two exponential curves with time constants $\tau_s = 7$ ns and $\tau_{ta} = 4.8$ μs. By increasing the temperature, the fast component decreases and disappears around 200 K keeping the same time constant, while the time constant of the slow component remains constant up to 60 K and then decreases down to 0.3 μs at room temperature. The results for the slow components are shown in Fig. 2. For temperatures lower than 60 K, the decay times show the characteristic behavior of the unthermalized triplet state [7].

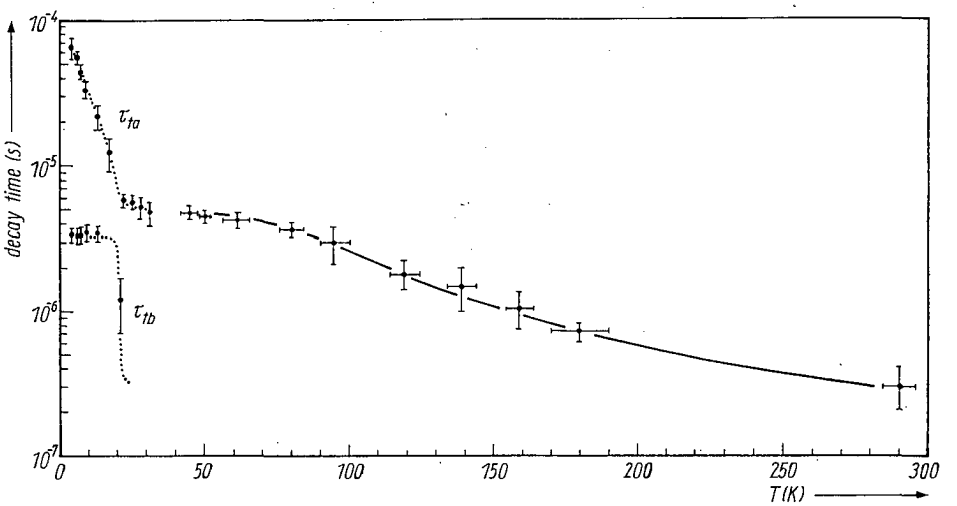

Fig. 2. Decay times of the 420 nm emission, under UV excitation of CsI:Na, as a function of the temperature. The solid line is obtained by assuming the one-phonon relaxation process between the triplet and the singlet levels and a non-radiative transition from the singlet level to the ground state. The dotted lines represent the fit given in [7]

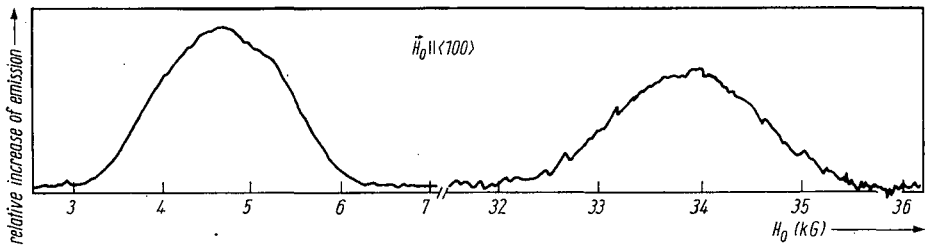

Fig. 3. ESR signals obtained by means of the optical detection on the 420 nm emission in CsI:Na at 1.4 K with the magnetic field parallel to the ⟨100⟩ direction and microwaves at 33.57 GHz. The sensitivity at 32 kG $< H_0 <$ 36 kG is 2.5 times larger than that at the lower field

The temperature dependence of the decay time constants of the 370 band is investigated up to 73 K [7]; their characteristics are the same as those of the 420 band except the absence of the fast decay with $\tau_s < 10^{-8}$ s.

3.4 Magneto-optical experiments

The ESR signals in Fig. 3 were observed by monitoring the 420 band under continuous UV excitation; $\boldsymbol{H}_0$ is applied parallel to ⟨100⟩. Each of these signals has approximately a Gaussian lineshape with a half-width of (1.70 ± 0.05) kG. The ESR signals with the same lineshape were also observed with X-band microwaves, at different values of $\boldsymbol{H}_0$ applied along ⟨100⟩. On the other hand, no ESR signal was found in either X or Q bands when $\boldsymbol{H}_0$ is applied along a ⟨110⟩ direction. Detecting on the 370 band, we found no ESR signal in both X and Q bands.

In Fig. 4, the magnetic field dependence of the MCP (MCP(H_0)) of the 420 band is given at several temperatures from 4.2 to 140 K. The MCP(H_0) shows a peak at 21.5 kG and another weak one around 4 kG at low temperature. The MCP(H_0) of the 370 band at 4.2 K is shown in Fig. 5. It increases smoothly when the magnetic field increases. No peak like the one observed in the case of the 420 band was found up to 50 kG.

The MCP was measured also as a function of the emission wavelength in both 370 and 420 bands at fixed H_0; the result is shown in Fig. 1a. The MCP intensity is constant in each band.

The magnetic field dependence of the slower decay time constant τ_{ta} was measured at 4.2 K for $\boldsymbol{H}_0$ along ⟨100⟩ by monitoring a circularly polarized 420 emission. τ_{ta} decreases monotonically with increasing H_0, with a weak dip around 22 kG.

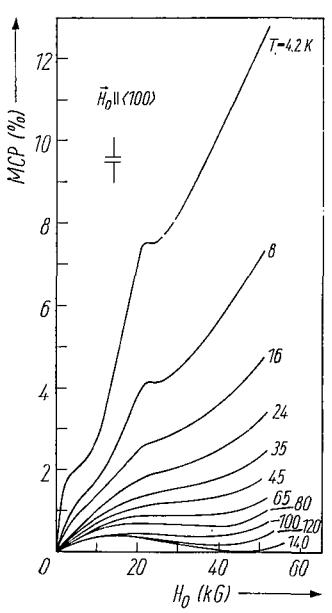

Fig. 4. Absolute MCP = $(I^- - I^+)/(I^- + I^+ + I)$ of 420 band in CsI:Na under the UV excitation at 234 nm and the magnetic field parallel to ⟨100⟩ direction

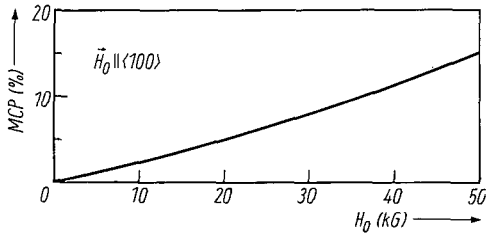

Fig. 5. Absolute MCP $= (I^- - I^+)/(I^- + I^+ + I)$ of the 370 band in CsI:Na at 4.2 K under the UV excitation at 237 nm and the magnetic field parallel to $\langle 100 \rangle$ direction

4. Model

We adopt a phenomenological model similar to that used in [7]. The electronic level scheme is given in Fig. 6a; the singlet level does not intervene for the 370 band. A σ-dipole transition occurs from the singlet level 4 and a multiplicity-forbidden π-transition from the triplet state (levels 2 and 3) takes place because of the singlet mixture through the spin–orbit coupling. E_{st} is the average energy separation between singlet and triplet states. The zero-field splittings in the triplet state are denoted D and E, as it will be seen in (1).

When $\boldsymbol{H}_0$ is applied along the z-direction and $g\beta H_0 \ll E_{st}$, the triplet state can be described by the following effective spin Hamiltonian:

$$\mathcal{H} = g_z \beta H_0 S_z + D\,[S_z^2 - \tfrac{1}{3} S(S+1)] + E(S_x^2 - S_y^2)\,. \tag{1}$$

In this equation, the third term is zero when the system has axial symmetry. The z-direction is parallel to the $\langle 100 \rangle$ crystal axis in the case of the self-trapped excitons in CsI.

The kinetics of the exciton with the energy levels shown in Fig. 6a can be described by four coupled rate equations

$$\frac{\mathrm{d}n_i}{\mathrm{d}t} = \sum_{j=1}^{4} C_{ij} n_j + R_i\,, \tag{2}$$

where $i = 1, 2, 3$, and 4, n_i is the occupation probability of level i at time t and R_i is its creation rate. The rate constants C_{ij} involve the spin relaxation and the radiative transition rates [11].

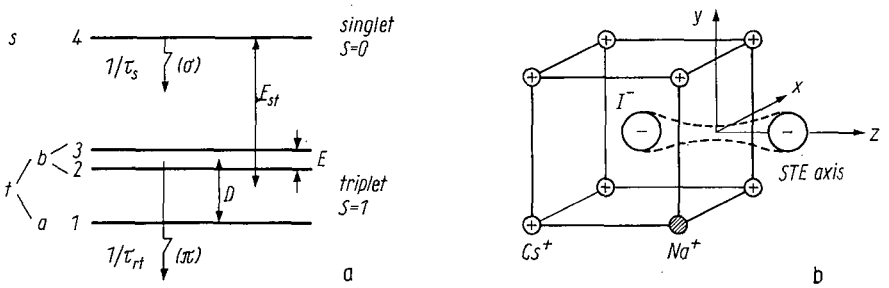

Fig. 6. a) Electronic levels scheme of a localized exciton. The ground state is singlet. Energy is not to scale. Detailed structure in the triplet state is simplified depending on the temperature of the excitons. b) Probable position of Na^+ ion in the cluster of the STE perturbed by Na^+ in CsI crystal

5. Analysis

5.1 420 band

The parameters g_z, D, and E in (1) have been determined using the four ESR signals botained in both X and Q bands; they are shown in Table 1. It must be pointed out that the consistent fitting of these four data was possible only for the case with $E \neq 0$ and the z-direction parallel to $\langle 100 \rangle$ axis.

Table 1

Values of the different parameters (see text) obtained from the analysis of the experimental data on the 420 emission band

D (eV)	$\lvert E \rvert$ (eV)	g_z	E_{st} (eV)	τ_{rb} (s)	τ_{rt} (s)	τ_s (s)	E_{nr} (eV)	τ_{nr} (s)
2.4×10^{-4}	5.5×10^{-5}	1.87	3.5×10^{-2}	3.3×10^{-6}	4.8×10^{-6}	7×10^{-9}	3×10^{-2}	1×10^{-8}

The fact that the unique triplet decay time constant does not vary (4.8 μs) between 30 and 60 K indicates that the triplet state is decoupled from the singlet state; the four coupled equations in (2) can then be decoupled to one equation for the singlet and to three equations for the triplet state. In [7], the dependence of the triplet decay times, on the temperature below 60 K, has been analyzed in terms of two coupled rate equations where the levels 2 and 3 in Fig. 6a are treated as a degenerated level whose lifetime is τ_{rb}; the contribution from two-phonon relaxation process was also pointed out. The value of D chosen for the fit is the same, within experimental error, as that obtained by ESR and shown in Table 1. The dotted lines in Fig. 2 represent this fit [7]. Although we have confirmed that $E \neq 0$, the analysis shown in [7] is still reasonable if one takes into account the experimental accuracy. We can have better fit of decay curves by assuming three decay time constants as theoretically expected. However, two of them $(\tau_{t2} = (3.3 \pm 0.3)\ \mu s$ and $\tau_{t3} = (2.9 \pm 0.3)\ \mu s$ at $4.2\ K)$ are the same within experimental error.

When the temperature is higher than 60 K, τ_{ta} decreases with increasing temperature. This may be due to a depopulation process from the triplet levels through the singlet level to which the excitation is induced by phonons. In order to analyze the decay times in this temperature region, the rate equations in (2) are simplified by considering the triplet state as a triply degenerate level whose lifetime is τ_{rt}; the one-phonon relaxation process is assumed between the triplet and singlet levels. A non-radiative transition probability from the singlet level to the ground state $((1/\tau_{nr}) \times \times \exp(-E_{nr}/kT))$ is added since the singlet component disappears for $T > 200$ K. The solid line in Fig. 2. is the theoretical curve obtained in this manner; values of fitting parameters are listed in Table 1.

As one can see from (1), the level crossing occurs between levels 1 and 2 when $\boldsymbol{H}_0$ is applied parallel to the z-axis. Anomaly in MCP(H_0) and $\tau_{ta}(H_0)$ may occur around the level crossing. Experimental data of MCP(H_0) and $\tau_{ta}(H_0)$ are qualitatively consistent with the model and parameters obtained so far. The analysis of these data, at low temperature, have been tried by adopting the model [11] where a local magnetic field is introduced to represent the hyperfine interaction in (1). This explains well the peak of MCP(H_0) and the dip of $\tau_{ta}(H_0)$ around the crossing but does not predict the small peak of MCP at 4 kG; this one is probably due to the magnetic field dependence of the creation process of excitons.

5.2 370 band

The tentative analysis of the temperature dependence of the decay times [7] gave a lifetime $\tau_{rb} = 1.7$ μs and $D = 2 \times 10^{-3}$ eV by assuming the one-phonon relaxation process. As for the zero-field splitting, however, the value would not be consistent with the fact that the triplet state is in thermal equilibrium above 15 K, where a unique exponential decay is observed. The relaxation rate between levels with such a large splitting (2 meV) would not be fast enough at 15 K to maintain the thermal equilibrium competing with the radiative process. This inconsistency is due to the contribution of the two-phonon process.

We saw neither ESR signal nor peaks of MCP up to 52 kG. This does not mean necessarily that no level crossing occurs in this magnetic field region [11]. Therefore, the determination of D and E remains for future work.

The decrease of the unique triplet decay time constant at $T > 30$ K together with the decrease of the 370 emission intensity suggest a contribution of a non-radiative process from the triplet state in this temperature region.

6. Discussion

6.1 420 band

The observation of the ESR was possible only when $\boldsymbol{H}_0$ was along a ⟨100⟩ direction. Furthermore, the anomalies of MCP($\boldsymbol{H}_0$) and $\tau_{ta}(\boldsymbol{H}_0)$ were observed for the case that $\boldsymbol{H}_0$ is parallel to ⟨100⟩. These two facts indicate that the system has the z-axis parallel or approximately parallel to a ⟨100⟩ direction. From the position of the excitation energy and the temperature dependence of decay times, we have proposed a localized exciton as the emitting center [7]. The fact that the z-axis is nearly parallel to ⟨100⟩ supports strongly this idea.

The parameter E in (1) is not zero. This indicates that x- and y-axis are not equivalent; the symmetry should be lower than D_{4h} which is the symmetry of the STE in CsI. From this results, one can say that the exciton is localized at an imperfection. The imperfection is probably a Na^+ impurity ion.

From the study of the absorption band at 717 nm in X-irradiated CsI:Na crystal [12], the presence of a Na atom located at the substitutional on-center or off-center positions is deduced. If we could adopt the result of the Na atom for the localized exciton, the most probable ionic structure might be the structure shown in Fig. 6b.

The width of the ESR line (1.7 kG) is consistent with the value estimated from those of F and V_k centers in CsI, as it was done for the STE in other alkali halide crystals [13]. Furthermore the similarity between the MCP of 338 and 420 bands suggests the similarity of their magnetic structure [11] except that the exchange energy for the 420 band is smaller than the one for the 338 band. According to our study of the recombination emission in CsI:Rb and CsI:K, one can notice the systematic energy shift in the emission of those crystals: 338 nm in CsI, 350 nm in CsI:Rb, 370 nm in CsI:K. We could consider the 420 band as an extension of this series. These results suggest a correspondence between the 338 band in CsI and the 420 band in CsI:Na, as it was pointed out in [14]. The 338 band involves only the triplet state, while the 420 band involves both singlet and triplet states. However, according to the model developed by Iida et al. [4], the exciton which is responsible of the 338 band should involve both singlet and triplet states. Therefore, this difference could be due to different ionic configurations between those centers in the relaxed states.

Since several models have been proposed for the origin of the 420 band, we have checked the possibility that this band would be composed of several different bands by measuring, for example, the wavelength dependence of MCP in the 420 band, as shown in Fig. 1b. Our experimental results do not support the idea.

6.2 370 band

In [7], we investigated the absorption, excitation, and emission associated with K^+ ions in CsI:K. In this case the characteristic emission occurs at 370 nm. The nature of the 370 band in each of CsI:Na and CsI:K crystals is different. The main differences are (i) in the absorption and excitation spectra which are at higher energy in CsI:K, (ii) the peak position and the half-width of the emission bands, and (iii) the existence of a singlet decay of the 370 band in CsI:K. This singlet component is evident at 70 K and grows by increasing the temperature.

The excitation spectra of 370 and 420 bands in CsI:Na are not the same, while the 290 and 338 bands in CsI have the same excitation spectrum [15]. This fact suggests that the relation between the 370 and 420 bands would be different from that between the 290 and 338 bands, or type I and type II excitons in CsI obtained by the theoretical model in [4].

7. Conclusion

The nature of the 420 emission in CsI:Na has been determined. This emission is a single band due to a triplet + singlet exciton localized at an imperfection with a symmetry lower than D_{4h}. The ionic structure could be described by the cluster of the STE in CsI where a Cs^+ ion is replaced by a Na^+ ion.

Acknowledgements

The authors are indebted to Dr. A. M. Stoneham and Prof. C. Jaccard for their discussions. They wish to thank Mr. J. P. Bourquin and Mr. F. Châtelain for their help in the construction of the flash lamp. This work has been supported by the Swiss National Science Foundation.

References

[1] H. LAMATSCH, J. ROSSEL, and E. SAURER, phys. stat. sol. (b) **48**, 311 (1971).
[2] L. FALCO, J. P. VON DER WEID, M. A. AEGERTER, T. IIDA, and Y. NAKAOKA, J. Phys. C **13**, 993 (1980).
[3] J. P. PELLAUX, T. IIDA, J. P. VON DER WEID, and M. A. AEGERTER, J. Phys. C **13**, 1009 (1980).
[4] T. IIDA, Y. NAKAOKA, J. P. VON DER WEID, and M. A. AEGERTER, J. Phys. C **13**, 983 (1980).
[5] Y. NAKAOKA and T. IIDA, phys. stat. sol. (b) **102**, 509 (1980).
[6] A. N. PANOVA and N. V. SHIRAN, Bull. Acad. Sci. URSS, Phys. Ser. **31**, 866 (1967).
[7] A. H. KAYAL, Y. MORI, C. JACCARD, and J. ROSSEL, Solid State Commun. **35**, 457 (1980).
[8] O. THIÉBAUD, J. J. PILLOUD, M. A. AEGERTER, and C. JACCARD, J. Physique C-7, 169 (1976).
[9] A. H. KAYAL, K. IMANAKA, and A. MEZGER, Solid State Commun., in the press.
[10] A. H. KAYAL, Ph.D. Thesis, Neuchâtel University, 1981.
[11] Y. MORI, C. JACCARD, J. P. VON DER WEID, and M. A. AEGERTER, J. Physique C-6, 443 (1980).
[12] Y. MORI, A. H. KAYAL, and C. JACCARD, Solid State Commun., to be published.
[13] D. BLOCK, A. WASIELA, and Y. MERLE D'AUBIGNÉ, J. Phys. C **11**, 4201 (1978).
[14] C. K. ONG, K. S. SONG, R. MONNIER, and A. M. STONEHAM, J. Phys. C **12**, 4641 (1979).
[15] H. LAMATSCH, J. ROSSEL, and E. SAURER, phys. stat. sol. **41**, 605 (1970).

(Received October 8, 1981)

phys. stat. sol. (b) 108, 449 (1981)

Subject classification: 13.5.1 and 20.3; 22.5.2

Institut de Physique, Université de Neuchâtel[1])

Self-Trapped Exciton Luminescence after Tunnelling of V_k and Na^0 Centers in CsI:Na Crystals

By

K. IMANAKA, A.-H. KAYAL, A. C. MEZGER, and J. ROSSEL

Tunnelling recombination luminescence in CsI:Na crystals is studied by means of linear polarization, magnetic circular polarization, and optical detection of ESR either under or after X-ray irradiation. Results are well interpreted in terms of a self-trapped exciton (STE) scheme as the final emitting state of tunnelling recombination; here, in the present case with tunnelling, the population for each STE sublevel is derived from the thermal equilibrium spin populations of trapped electrons (Na^0) and holes (V_k) instead of the usual creation rate in UV light excitation case.

La luminescence de recombinaison après un transfert par effet tunnel est étudiée dans un cristal de CsI:Na à l'aide de la polarisation linéaire, de la polarisation magnétique circulaire et de la détection optique de la RPE soit sous irradiation par RX soit après irradiation. Les résultats peuvent être interprétés par un modèle d'exciton autopiégé (STE) créé après un transfert par effet tunnel; dans le cas présent, la population de chaque sous-niveau de l'exciton est calculée à partir des populations de spin d'un électron piégé (Na^0) et d'un trou (V_k) en équilibre thermique au lieu du calcul usuel à partir de la probabilité de création dans le cas d'une excitation UV.

1. Introduction

In spite of a number of studies on the tunnelling recombination luminescence of trapped hole (V_k) and trapped electron (M^0) centers in alkali halides doped with impurity ions M^+ [1 to 3], very little is known on the emitting state after tunnelling. In this report, by a study of CsI:Na crystals as one of examples, we propose that the recombination luminescence occurs via the self-trapped exciton (STE) state perturbed by an M^+ ion after tunnelling, since in this crystal the emission band peak ($\approx$ 420 nm) and halfwidth under or after X-ray irradiation are almost the same as those by UV light excitation [4].

Magneto-optical properties of the 420 nm band in CsI:Na have been studied extensively in our laboratory by UV excitation [5] and by X-ray irradiation [6, 7]. In the latter work, some ESR signals in the 420 nm emission with X-band μ-wave have been observed, which are not seen in the UV excitation case and whose resonance positions seem to correspond to the resonance at V_k centers [8]. By this result, we suspect that the STE preserves a memory of paramagnetic centers, V_k and Na^0, which will be recombined by tunnelling. On the basis of this hypothesis, we introduce thermal equilibrium spin populations of each center as the population of the STE state.

To confirm these ideas, we measured linear polarization (LP) (preliminary measurements have been done in [9]), magnetic circular polarization (MCP), and ESR optically with Q-band μ-wave, in emission. These experimental procedures and results are given in Section 2. In Section 3, an STE scheme is calculated approximately in D_{4h} symmetry. Section 4 is devoted to comparison with experiments and discussions.

[1]) 2000 Neuchâtel, Switzerland.

2. Experimental Procedure and Results

Single crystals of CsI doped with Na^+ impurities ($\approx$ 200 ppm) were cut into suitable sizes with all surfaces being (100) oriented, and were annealed at about 450 °C for one day in order to get rid of internal strains which depolarized the emitted light. Then, the specimens were mounted on a sample holder in a flow-type cryostat for the LP measurement, or in a superconducting split-coil cryostat for the MCP; in the case of optical detection of ESR, the sample was placed on the bottom of a TE_{111} Q-band μ-wave cavity. The 420 nm emission was obtained under or after X-ray irradiation from a tungsten-target tube operating at 150 kV/10 mA, and detected by a photomultiplier (EMI 9558 QB) through a monochromator or appropriate broad band pass filters.

In some of measurements, we stimulated an IR absorption band of Na^0 centers to liberate electrons from the trap centers [10]. By this method, the 338 nm intrinsic luminescence of CsI was induced through the recombination of an electron and V_k center [10, 11], and the 420 nm tunnelling recombination was stimulated: When we measured the emission using chopped IR light ($\approx$ 100 Hz) with a lock-in amplifier or using cw IR light with an ammeter, the 338 nm emission intensity did not change in both cases, but the 420 nm emission was too small to be detected in the former case. In all measurements, the emission was detected along the $\langle 100 \rangle$ crystalline axis (z-direction).

2.1 Linear polarization

After X-ray irradiation at temperature lower than 40 K, V_k centers were almost completely aligned to the [010] (y-) direction perpendicular to the detection axis by illumination with unpolarized V_k excitation light ($\approx$ 410 nm) from a Hg lamp (HBO 200) with appropriate filters. Then, the LP of emission was measured by using a rotating linear polarizer and a lock-in amplifier. A schematic diagram for this measurement is shown in Fig. 1a. An experimental result is shown in Fig. 2a, where $I_{\parallel}$ and $I_{\perp}$ represent emission intensities polarized parallel and perpendicular to the aligned V_k center axis, respectively. In these measurements, we stimulated the IR band of Na^0 in order to emphasize contrast between thc 420 nm band and the intrinsic luminescence of CsI pure exciton (338 nm, π-polarized) [11], since no tunnelling recombination luminescence of 338 nm was observed. The solid curve in Fig. 2a gives the value of LP defined by $(I_{\parallel} - I_{\perp})/(I_{\parallel} + I_{\perp})$; these data were corrected for the

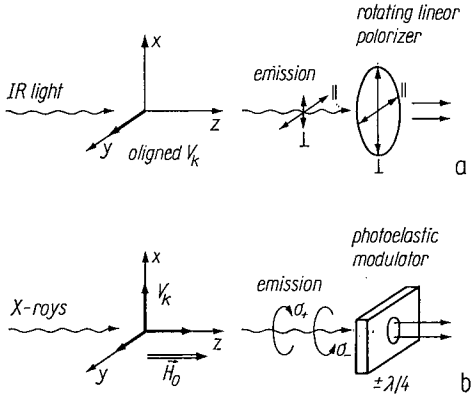

Fig. 1. Schematic diagrams of measurements for a) linear polarization and b) magnetic circular polarization

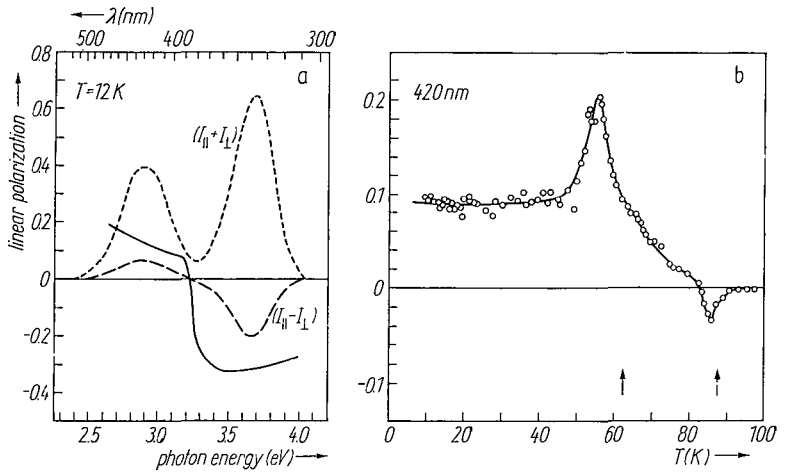

Fig. 2. Experimental results of a) linear polarization of emission for 420 and 338 nm bands (solid lines give the corrected LP) and b) temperature dependence of LP for 420 nm emission (arrows indicate thermoluminescence peaks)

polarization effects of the measuring system by using data of LP under X-rays without V_k alignment. We can see clearly the σ-polarized character for the 420 nm band contrary to the π-character for the 338 nm band. This result suggests that the 420 nm band contains the emission from the singlet state. In Fig. 2b, the temperature dependence of LP for the 420 nm band is depicted; in this measurement, we did not stimulate the IR band of Na^0 in order to avoid rapid bleaching of centers. It shows a peak at around 55 K followed by a rapid decrease until reaching negative values above this temperature. Thermoluminescence peaks [12] are also indicated by arrows for discussions.

2.2 Magnetic circular polarization

The magnetic circular polarization of 420 nm emission was measured under X-rays by using a photoelastic modulator (Hinds) with the magnetic field, $\boldsymbol{H}_0$, parallel to the z-axis for $0 < H_0 < 50$ kOe at 1.6 K $< T <$ 80 K; here, we define the MCP by $(I_{\sigma_-} - I_{\sigma_+})/I_t(H_0)$, where I_{σ_-} and I_{σ_+} are circularly polarized intensities of emission, and $I_t(H_0)$ is the total emission intensity. A schematic diagram for this measurement is shown in Fig. 1b. Experimental results are shown in Fig. 3 by solid curves. This result suggests that the triplet state is also involved in the 420 nm band. However, absolute values of MCP are much smaller than those obtained for the intrinsic luminescence of CsI at the same temperature [11]. This fact supports that the singlet state is also contained in the 420 nm band as mentioned in the LP result, since the emission from the singlet state contributes only to the denominator of MCP, $I_t(H_0)$.

A result of MCP by UV excitation (230 nm) at 4.2 K [5] is also shown in Fig. 3 by dashed curves in order to clarify the identity of emitting state in these two cases of the present tunnelling recombination and the STE luminescence by UV excitation. Results show similar behavior under both X-rays and UV, but curves are rather simpler in the X-ray case; especially, the peak at around 21 kOe in UV case, which is assigned to be due to level crossing in the triplet state [4, 5], is not so apparent in the X-ray case. This fact implies that populations in STE sublevels are different in the X-ray and UV cases. Details will be discussed later.

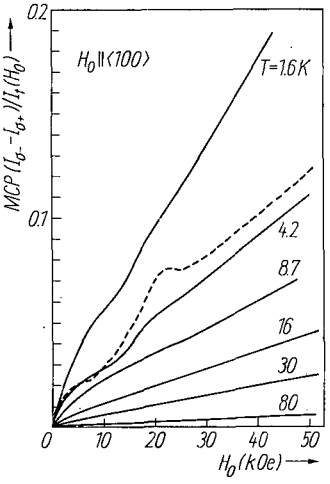

Fig. 3. Experimental results of the MCP as a function of magnetic field and temperature for 420 nm band. Dashed line shows the MCP obtained by UV excitation at 4.2 K. ——— under X-rays, — — — under UV

2.3 Optical detection of ESR

The Q-band μ-wave transition was observed optically via the 420 nm emission at 1.5 K by using two methods with the magnetic field being parallel to the ⟨100⟩ crystalline axis (*z*-direction); a) by monitoring changes in the total emission intensity with chopped μ-wave (≈ 40 Hz), and b) by monitoring the MCP with cw μ-wave. Experimental results are shown in Fig. 4 a and b for the cases a and b, respectively. Here, we used X-rays and IR light simultaneously as excitation and stimulation to enhance the signal-to-noise ratio, since at these low temperatures, trapped centers were rather stable. Resonance frequencies were calibrated by setting DPPH inside the cavity with the sample. These ESR signals cannot be observed in the UV excitation case. On each figure, we can see one sharp resonance peak at the lower magnetic field side and a rather broad signal at higher field. These signals do not seem to have Gaussian lineshapes; this is not unreasonable when the resonance occurs in a trapped hole or in a trapped electron. By a theoretical inference described later, the resonance

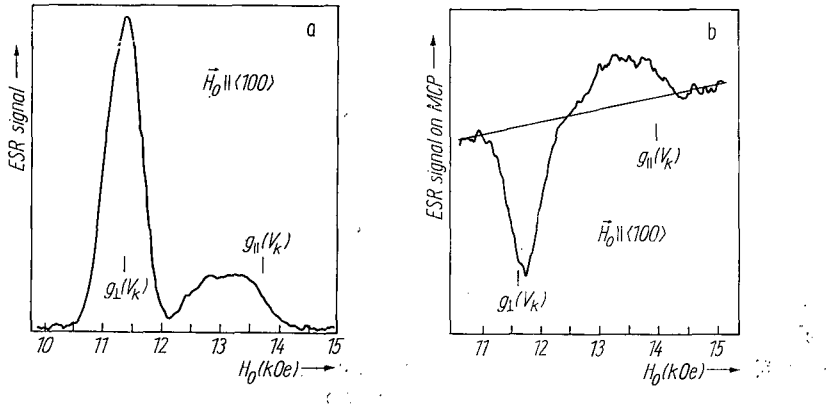

Fig. 4. a) ESR signal obtained by monitoring the change in total emission intensity and b) ESR signal on the MCP. $T = 1.5$ K, $\nu = 36.3$ GHz, for a) and 36.9 GHz for b), 420 nm band

positions for the V_k center are indicated by arrows with g-values of $g_\perp(V_k) = 2.27$ for $V_k \perp \boldsymbol{H}_0$, and $g_{||}(V_k) = 1.89$ for $V_k \,||\, \boldsymbol{H}_0$ determined by the electronic detection [8]. We can see the sharp resonance peaks located at almost the same position of $V_k \perp \boldsymbol{H}_0$.

3. Model

3.1 STE state

First, we introduce an STE scheme for the 420 nm band by the same method as developed by Iida et al. [11] or Fowler et al. [13] for the STE in D_{4h} symmetry. Strictly speaking, we must consider a lower symmetry than D_{4h} due to the Na^+ impurity. However, for the moment no experimental information on the position of Na^+ ion has been given; only theoretically, the most probable position is predicted to be one of substitutional sites of Cs^+ ions at nearest neighbors to V_k center [14, 15]. Therefore, as a zeroth-order approximation, we assume that four Cs^+ ions (or three Cs^+ + one Na^+) are not deformed much by Na^+ impurity, and on these ions a 3s electron originating from Na^0 center exists as a partner of STE preserving D_{4h} symmetry. When we could find out where Na^+ is, we could introduce an effect due to the impurity by an appropriate perturbation to our scheme.

By using the following parameters determined by Iida et al. for the 338 nm emission of the CsI pure exciton [11], energy levels and wave function of STE are computed numerically by diagonalizing the spin–orbit and Zeeman interactions; $E = 1.88$ eV (which corresponds to $E_{15} - E_{12}$ in Iida's definition, and to C in Fowler's), $\lambda = 0.584$ eV (spin–orbit coupling constant), and $L_{||} = 0.7$ and $L_\perp = 1.3$ (orbital quenching parameters). The most important difference is in the value of exchange energy; we used $J = 3.0$ meV (which corresponds to J_{12} in Iida's notation) instead of 9.0 meV so as to explain the zero-field splitting and the level crossing of triplet levels at around 21 kOe [4, 5]. A part of the calculated energy scheme for the lower lying four levels is shown in Fig. 5. On the left-hand side of the figure, the unperturbed state as the eigenstate of exchange and crystal field is depicted, where we classify the state in the same way as Fowler did [13]. In the STE scheme, $|s^\eta\rangle$ represents the singlet state of $(S, S_z) = (0, 0)$, and $|+^\eta\rangle$, $|0^\eta\rangle$, and $|-^\eta\rangle$ the triplet states of (1, 1), (1, 0), and (1, −1),

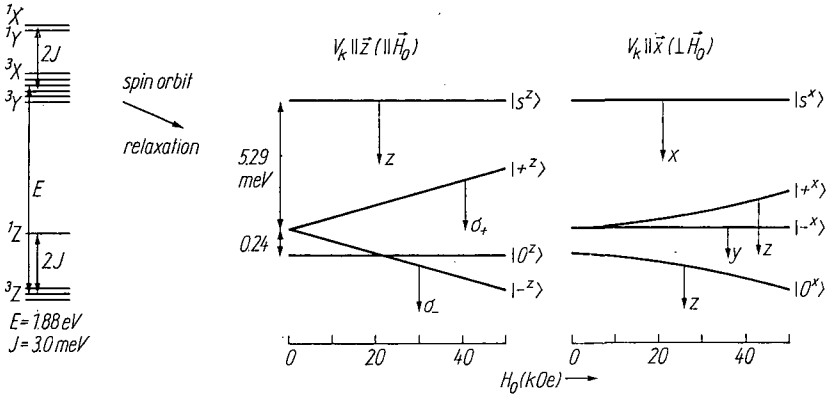

Fig. 5. Calculated energy scheme of the STE state; the scheme for $V_k \,||\, \boldsymbol{y}$ is obtained by replacing x by y in the case for $V_k \,||\, \boldsymbol{x}$

respectively, where η (= x, y, or z) stands for the direction of STE axis corresponding to the V_k axis in this case and being parallel (z) to or perpendicular (x, y) to the applied magnetic field. The polarizations of emitted light are also shown by x, y, z, σ_+, and σ_-.

3.2 Population of STE state

As in the case of the usual STE model, we assume that the STE levels are not in thermal equilibrium. However, by the results of ESR shown in Fig. 4 a and b, we suppose that the STE preserves a memory of paramagnetic centers, V_k and Na^0, prior to the recombination in the present tunnelling case; before tunnelling, these centers are rather stable and the thermal equilibrium is attained [8, 10, 16, 17]. On the basis of this hypothesis, we derive the population N_ζ^η for each STE level, $|\zeta^\eta\rangle$, in the following way. When we define thermal equilibrium spin population of V_k and Na^0 in the ground Zeeman sublevels, i.e. Boltzmann distribution, by $n_v^\eta(\uparrow\downarrow)$ and $n_e(\uparrow\downarrow)$, where $\uparrow$ and $\downarrow$ represent the spin-up and spin-down states, respectively, we can approximately express the population of a virtual pair (or coupled) state of two particles after tunnelling before relaxation by

$$\begin{aligned} n_S^\eta &= \tfrac{1}{2}\,[n_v^\eta(\uparrow)\, n_e(\downarrow) + n_v^\eta(\downarrow)\, n_e(\uparrow)] = n_0^\eta\,, \\ n_+^\eta &= n_v^\eta(\uparrow)\, n_e(\uparrow)\,, \\ n_-^\eta &= n_v^\eta(\downarrow)\, n_e(\downarrow)\,, \end{aligned} \tag{1}$$

where η stands for the direction of STE axis being parallel ($\|$) or perpendicular ($\perp$) to the applied magnetic field. To simplify the problem, we assume an isotropic g-value for Na^0 as in the case of Ag^0 center [16, 17]. Equation (1) was justified in terms of a density matrix calculation. Just after the pair state, the electron and hole relax to the STE state with relaxation rates W_S (for singlet) and W_T (for triplet). Then, we can get the population of STE levels as

$$N_S^\eta = W_S n_S^\eta\,, \quad \text{and} \quad N_\zeta^\eta = W_T n_\zeta^\eta \qquad (\zeta = +, 0, \text{and } -)\,. \tag{2}$$

3.3 Emission intensity

Now, using the wave functions and populations of the STE state obtained in the preceding subsections, we can calculate the ξ-polarized 420 nm emission intensity, I_ξ, by the product form of $\sum_{\zeta,\eta} I_\xi(\zeta^\eta)\, N_\zeta^\eta$, where $I_\xi(\zeta^\eta)$ represents the ξ-polarized component of zeroth moment for the $|\zeta^\eta\rangle$ state ($\eta = x(\perp)$, $y(\perp)$, and $z(\|)$, ζ = s, +, 0, and $-$). Then we can get theoretical forms for experimentally obtained quantities as follows with taking into account the emission from the singlet state.

3.3.1 LP

When the V_k center is aligned to the y-direction and the emission is observed along the z-direction, we can derive a theoretical form of the LP in the same manner as Iida et al. [11]. Without magnetic field, the population of each STE level in our scheme is given by $W_S/4$ for singlet and $W_T/4$ for triplet states by putting $H_0 = 0$ in (1) and (2). Thus, the LP defined by $(I_\| - I_\perp)/(I_\| + I_\perp) = (I_y - I_x)/(I_y + I_x)$ is given by

$$\mathrm{LP} = \frac{(1-\delta)\,(1-A)}{(1+\delta) + (1+3\delta)\,A} \tag{3}$$

with

$$A = \frac{\tau_S}{\tau_T}\,\frac{W_T}{W_S}\,; \tag{4}$$

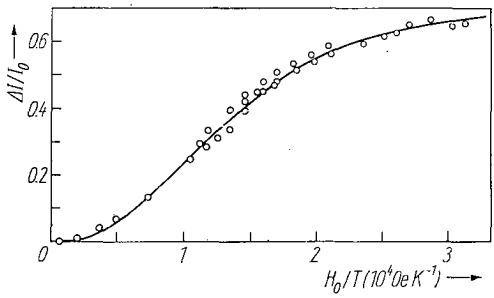

Fig. 6. Relative change in emission intensity due to magnetic field. Circles are the experimental results after [2], and solid curve shows theoretically best-fitted ones. g (Na^0) = 1.99, $W_T\tau_S/W_S\tau_T = 0.054$.

here we put $I_y(s^y) = I_x(s^x) = 1/\tau_S$ and $I_x(+^z) = I_y(-^z) = I_y(-^x) = I_x(-^y) = 1/\tau_T$, and δ represents the ratio of the number of STE oriented along the x- or z-direction to that along the y-direction when they emit photons, which has been defined by Iida et al. [11] and determined to be $\delta = 0.39$ in CsI pure excitons.

3.3.2 MCP

When a magnetic field $\boldsymbol{H}_0$ is applied in z-direction, only the STE oriented along the z-axis emits circularly polarized light when observed along the z-direction; therefore, the emission intensity of circularly polarized light is given by

$$I_\xi = \sum_{\zeta=+,-} I_\xi(\zeta^z)\, W_T n_\zeta^{\parallel} \qquad (\xi = \sigma_+ \text{ and } \sigma_-)\,. \tag{5}$$

On the other hand, the total emission intensity is

$$I_t(H_0) = I_{\sigma+} + I_{\sigma-} + 2I_x(s^x)\, W_S n_S^{\perp} + 2I_y(-^x)\, W_T n_{\pm}^{\perp}\,. \tag{6}$$

Using (5) and (6), we can calculate the MCP by $(I_{\sigma-} - I_{\sigma+})/I_t(H_0)$ when we know W_S, W_T, and $g(Na^0)$.

3.3.3 Intensity change due to magnetic field

When a magnetic field is applied, the intensity of tunnelling recombination luminescence $I_t(H_0)$ decreases. A relative change in the intensity $\Delta I/I_0 = [I_t(0) - I_t(H_0)]/I_t(0)$ has been observed by Delbecq et al. for KCl:Ag [16] and by Thiébaud et al. for CsI:Na [2]. Results for CsI:Na are shown in Fig. 6 by circles. A theoretical form for this quantity is derived as follows in our STE scheme using (1), (2), (5), and (6),

$$\frac{\Delta I}{I_0} = 1 - \frac{A(n_+^{\parallel} + n_-^{\parallel}) + 2n_S^{\perp} + 2An_{\pm}^{\perp}}{(A + \frac{1}{2})}\,, \tag{7}$$

where A is defined in (4) and we used the following approximations: $I_{\sigma+}(\zeta^z) + I_{\sigma-}(\zeta^z) = I_y(-^x) = 1/\tau_T$ ($\zeta = +$ and $-$), and $I_x(s^x) = 1/\tau^S$, since changes in the zeroth moment due to magnetic field are small enough.

3.3.4 Optical detection of ESR

Qualitatively speaking, when the μ-wave transition occurs in Na^0, $V_k \perp \boldsymbol{H}_0$, or $V_k \parallel \boldsymbol{H}_0$, the population $n_e(\uparrow\downarrow)$, $n_\nabla^{\perp}(\uparrow\downarrow)$, or $n_\Downarrow^{\parallel}(\uparrow\downarrow)$ is altered, respectively, and this alteration causes the change in population of STE level N_ζ^η via the change in virtual population given in (1). Then, the emission intensity varies, since it is given by the product of zeroth moment and the population as shown in (5) and (6). Now, we can explain the ESR signal detected optically as follows: a) when the ESR is observed via the

change in intensity as shown in Fig. 4a, we should see the resonance signals at the resonance fields for $V_k \perp \boldsymbol{H}_0$, $V_k \parallel \boldsymbol{H}_0$, and Na^0, since we are detecting the change in the total emission intensity given in (6); and b), on the other hand, when the ESR is observed via the MCP as shown in Fig. 4b, we should see resonances at $V_k \parallel \boldsymbol{H}_0$ and Na^0 by (5) and $V_k \perp \boldsymbol{H}_0$ should not be observed in this case.

4. Comparison with Experiments and Discussion

Analyzing experimental results of $\Delta I/I_0$ shown in Fig. 6 through equation (7) with the aid of the method of least squares, we get $g(Na^0) \approx 1.99$ and $A \approx 0.054$; the best fitting theoretical curve is shown in Fig. 6 by the solid curve. Theoretical calculation of the STE scheme given in Fig. 5 gives $\tau_S/\tau_T \approx 0.0427$; thus, we can determine the ratio of W_T/W_S from (4) as 1.26. Now, using these parameters, we can evaluate the LP and the MCP.

By calculating (3), we can get the value of LP equal to 0.38. This value is rather large in comparison with our experimental results. This fact may imply that the STE axis is not the same as in the pure CsI case due to Na^+ impurity; another possibility is discussed later. As for the temperature dependence of LP, the first peak can be explained when we assume thermal equilibrium in the STE state at these temperatures, since when thermal equilibrium is attained, excitons populate more the singlet state and emit more strongly σ-polarized light. As can be seen in Fig. 5, the calculated energy separation between the singlet and the triplet states is about 5.3 meV ($\approx$ 61 K), which is close to the first peak temperature. Above this temperature, thermal reorientation of V_k centers starts to occur decreasing the LP until giving a negative value. This situation is confirmed by the results of LP in KCl:Ag and KCl:Tl observed by Delbecq et al. [1]; in these two crystals, the LP shows negative values at the same temperature in spite of the difference in doping impurity.

The MCP is calculated from (5) and (6) with $g(Na^0) = 1.99$, and results are shown in Fig. 7. Since we did not introduce any population exchange phenomenon [4, 5, 11, 13], which would be important around the level crossing point, no structure is seen in MCP: However, the agreement with experiments seems to be satisfactory.

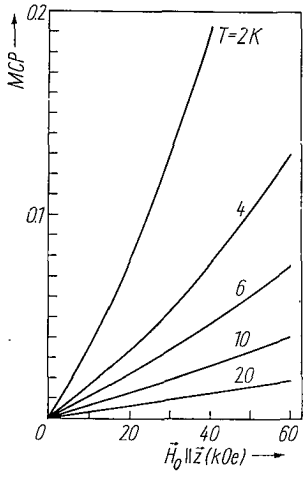

Fig. 7. Calculated MCP by putting g (Na^0) = 1.99

On the basis of the theoretical inference discussed in the preceding section, the ESR signals shown in Fig. 4 a and b can be assigned as follows. (i) The sharp resonance signal in each figure presumably corresponds to the resonance for $V_k \perp \boldsymbol{H}_0$. However, we cannot explain why the signal in this optical detection is not resolved due to the hyperfine interaction as has been observed by electronic detection [8]; such a situation also happens on F centers in alkali halide [18]. (ii) Rather broad resonance signals are attributed to a composition of resonance at $V_k \parallel \boldsymbol{H}_0$ and Na^0. However, precise decomposition of this signal is not so easy, since the resonance signal for $V_k \parallel \boldsymbol{H}_0$ and that for Na^0 have not Gaussian lineshapes and, moreover, the signal for $V_k \parallel \boldsymbol{H}_0$ must be small; we can detect the signal for $V_k \parallel \boldsymbol{H}_0$ only from the π-polarized component of luminescence from the STE $\parallel \boldsymbol{H}_0$.

However, as has been mentioned already, the $g_\perp(V_k)$ signal should not be observed in the MCP case. This anomalous signal leads us to introduce the reabsorption of 420 nm emission by the V_k center whose absorption peak is located at 408 nm. Since the 420 nm emission has a circularly polarized component under magnetic field, we may obtain an MCD signal of the V_k absorption band, and this phenomenon probably contributes to the MCP signal with negative sign; this can also explain why the resonance signal for $V_k \parallel \boldsymbol{H}_0$ is so small.

The existence of this reabsorption can explain the peak shift of the 420 nm band to the lower-energy side as seen by $(I_\parallel + I_\perp)$ in Fig. 2a and can be justified by the fact that the value of LP shown in Fig. 2a is smaller in the region of the V_k absorption band not only in the 420 nm band but also in the 338 nm band, since the V_k center absorbs the σ-polarized light $(I_\parallel)$.

We never talked about the dynamical mechanism of tunnelling; we believe it is worthwhile to discuss it here before closing this report. After X-ray irradiation on CsI:Na, no experimental evidence has been observed for the existence of a V_k center perturbed by an Na^+ ion $[V_k + Na^+]$, e.g. V_{kA} center [8, 12]. However, we cannot exclude the existence of a small amount of $[V_k + Na^+]$ which may be difficult to be observed in low doping levels of impurities. Thus, possible tunnelling processes which give the 420 nm recombination luminescence will be as follows: (i) an electron liberated from Na^0 tunnels to the $[V_k + Na^+]$ center, or (ii) a V_k center tunnels to an Na^0 center. The first process is excluded by the following reason: if the electron tunnels to $[V_k + Na^+]$, it must meet a V_k center with a larger probability, since the concentration of V_k must be much higher than that of $[V_k + Na^+]$. Thus, in this case, the 338 nm emission should be observed after X-ray irradiation contrary to the experimental result. Now, we believe the most probable process is the V_k tunnelling to Na^0. This opinion can be confirmed by the experimental result that when we excited the V_k band, we could stimulate the 420 nm luminescence after X-ray irradiation.

Acknowledgements

The authors are much indebted to Dr. Y. Mori, Dr. J.-J. Pilloud, and Prof. H. Beck for many helpful discussions, and one of the authors (K.I.) wishes to express his thanks to Prof. C. Jaccard and Prof. H. Ohkura who gave him the nice occasion to study in Neuchâtel as a post-doctoral fellow. This work is supported by the Swiss National Foundation for Scientific Research.

References

[1] C. J. Delbecq, Y. Toyozawa, and P. H. Yuster, Phys. Rev. B 9, 4497 (1974).
[2] O. Thiébaud, J.-J. Pilloud, M. A. Aegerter, and C. Jaccard, J. Physique C7, 169 (1976).
[3] T. Tashiro, S. Takeuchi, M. Saidoh, and N. Itoh, phys. stat. sol. (b) 92, 611 (1979).

[4] A.-H. KAYAL, Y. MORI, C. JACCARD, and J. ROSSEL, Solid State Commun. **35**, 457 (1980).
[5] A.-H. KAYAL, Y. MORI, and J. ROSSEL, to be submitted.
[6] J. P. VON DER WEID and M. A. AEGERTER, Solid State Commun. **27**, 519 (1978).
[7] J. P. VON DER WEID and M. A. AEGERTER, J. Lum. **18/19**, 858 (1979).
[8] J.-J. PILLOUD and C. JACCARD, Solid State Commun. **17**, 907 (1975).
[9] T. SIDLER, Ph. D. Thesis, Univ. of Neuchâtel (Switzerland), 1976.
[10] Y. MORI, A.-H. KAYAL, C. JACCARD, and M. A. AEGERTER, Solid State Commun. **34**, 315 (1980).
[11] T. IIDA, Y. NAKAOKA, J. P. VON DER WEID, and M. A. AEGERTER, J. Phys. C **13**, 983 (1980).
[12] T. SIDLER, J.-P. PELLAUX, A. NOUAILHAT, and M. A. AEGERTER, Solid State Commun. **13**, 479 (1973).
[13] W. B. FOWLER, M. J. MARRONE, and M. N. KABLER, Phys. Rev. **B 8**, 5909 (1973).
[14] C. K. ONG, K. S. SONG, R. MONNIER, and A. M. STONEHAM, J. Phys. C **12**, 4641 (1979).
[15] M. J. L. SANGSTER, J. Phys. C **13**, 5279 (1980).
[16] C. J. DELBECQ and P. H. YUSTER, phys. stat. sol. (b) **68**, K21 (1975).
[17] C. J. DELBECQ, W. HAYES, M. C. M. O'BRIEN, and P. H. YUSTER, Proc. Roy. Soc. **A271**, 243 (1963).
[18] H. J. REYHER, K. HAHN, TH. VETTER, and A. WINNACKER, Z. Phys. **B33**, 357 (1979).

(Received September 17, 1981)

Solid State Communications, Vol.35, pp.457-460.
Pergamon Press Ltd. 1980. Printed in Great Britain.

LUMINESCENCE PROCESSES IN CsI DOPED WITH Na^+ AND K^+ IONS

A.H. Kayal, Y. Mori*, C. Jaccard and J. Rossel

Institut de Physique, Université de Neuchâtel
CH-2000 Neuchâtel, Switzerland

(Received 26 March, 1980 by G. F. Bassani)

The luminescence bands around 420 nm and 370 nm in CsI:Na and CsI:K have been studied by measuring the temperature dependence of decay times and luminescence and its excitation spectra. The bands are due to singlet+triplet localized excitons and to triplet localized excitons, respectively, at low temperature. Zero field splitting and life time amount to 0.2 meV and 3.3 μs for the 420 nm band, and to 2.1 meV and 1.7 μs for the 370 nm band. Creation processes of 420 nm excitons may not be the same below 40 K and near room temperature.

Among several luminescence bands so far observed in the CsI crystal, there is an efficient blue luminescence around 420 nm associated with the Na^+ ions[1,2,3]. Even though the luminescence makes the crystal of CsI:Na a good X-ray scintillator[4], the mechanisms which lead to the blue luminescence are not clear. As a first step to understand them together with electronic and ionic structures involved in the luminescence, we have studied the luminescence, its excitation spectra, its decay time and their temperature dependence for crystals of CsI doped with Na^+ ions, as well as CsI doped with K^+ ions for comparison.

Crystals with different doping levels were grown by the Czochralski method in our laboratory from Merck "Suprapur" powder. The luminescence was excited by a D_2 lamp or by a W-target X-ray source operating at 150 KV, 12 mA, or a home made nanosecond pulse discharge D_2 lamp through a Leitz prism monochromator, it was detected by a cooled photomultiplier (RCA C31000 M) through another Leitz prism monochromator followed by a DC current meter, or by a time resolved one-photon detection system fast enough with respect to the typical value of the light pulse width (7 ns).

Fig. 1 (curve a) and (curve b) shows the luminescence spectra of CsI:Na and CsI:K under X-ray excitation at 20 K. In these crystals, the luminescence bands occur around 420 nm and 370 nm respectively, together with the intrinsic luminescence peaked at 338 nm. Under UV excitation near the intrinsic absorption edge, similar bands (called 420 and 370 bands) have been also observed, as shown in Fig. 2 (curve a) and (curve b)[5]; the absorption and excitation spectra for 420 and 370 bands in CsI:Na and CsI:K are shown in Fig. 3. The peak position and half-width ΔE of these bands are slightly temperature dependent : the 420 band shifts from 416±4 nm, ΔE = 0.33±0.03 eV at 4.2 K to 430±4 nm, ΔE = 0.67±0.03 eV at 300 K and the 370 band from 373±4 nm, ΔE = 0.39±0.03 eV at 10 K to 381±4 nm, ΔE = 0.61±0.03 eV at 150 K. The 370 band and the absorption related to the luminescence might be associated with K^+ ions as has been pointed out by Panova and Shiran[2].

The luminescence decay of the 420 and 370 bands after UV pulse excitation at 73 K is composed of two exponential curves with time constants of 4.2 μsec and less than 10 nsec and a single exponential of 0.7 μsec, respectively. These results, together with their temperature dependence shown later, suggest that the 370 band is due to a triplet exciton and that the 420 band is due to both singlet and triplet excitons at low temperature. The singlet component of the 420 band disappears at RT and the triplet components in both bands split into two components at low temperature.

The temperature dependence of the decay time of both bands is shown in Fig. 4 (a) and (b)[6]. The characteristic behaviour below 20 K for the 370 band is similar to that observed for the intrinsic luminescence in KI[7]; it has been explained with the model in Fig. 5 in which the relaxation rates P_a and P_b are determined by a one-phonon process. The solid line in Fig. 4(a) was calculated by using the same equation as in the case of KI. The fitting parameters for the solid line are E_{ba} = 1.9 meV, τ_{rb} = 1.7 μsec, $\tau_{ra} = \infty$, τ_{oa} = 0.13 μsec, τ_{ob} = 1 μsec; the set of parameters must be confirmed by magnetic circular polarization (MCP) and electron spin resonance (ESR) because of the problem shown below.

The temperature dependence of the 420 band can also be analyzed in terms of the same model by introducing a non-zero radiative rate from level a and an energy difference E_{ba} of 2.0 meV. However preliminary results of MCP of the 420 band show a weak peak at 22 KG which may probably be due to the crossing between a sublevel of b and the level a; the magnetic field of 22 KG implies an energy E_{ba} of about 10 times smaller (∿0.2 meV). This disagreement may be due to the assumption of an one-phonon process valid

* On leave from Department of Applied Physics, Osaka City University, Osaka, Japan

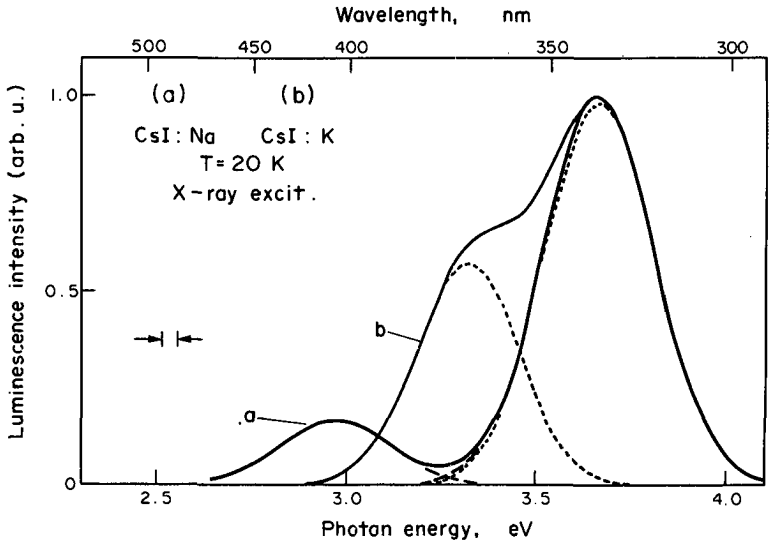

Fig. 1 (a) and (b)
The luminescence spectra of CsI:Na (a) and CsI:K (b) under X-ray excitation at 20 K. The experimental results (solid lines) are decomposed into two symmetric gaussians (broken lines) by fitting at 338 nm the peak position of the intrinsic luminescence.

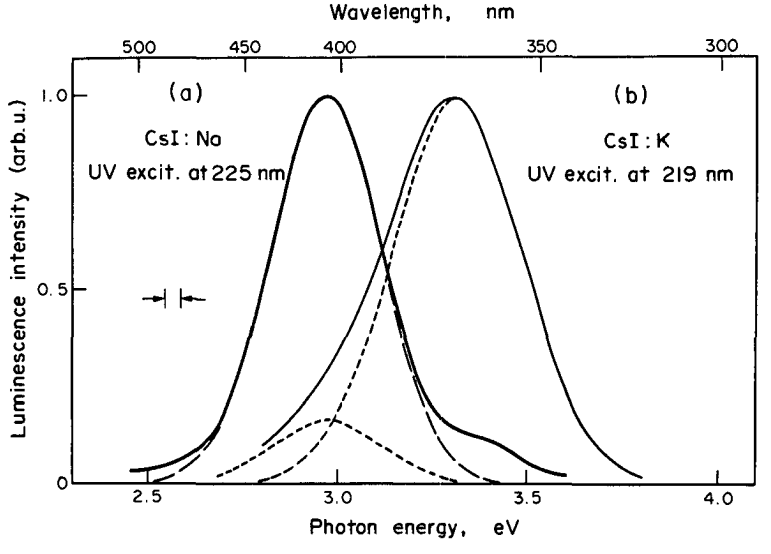

Fig. 2 (a) and (b)
The luminescence spectra of CsI:Na (a) and CsI:K (b) at 12 K under UV excitation in the absorption bands near the intrinsic absorption edge. The experimental spectra obtained (solid lines) are fitted with two symmetric gaussians (broken lines).

at all temperatures. Indeed the slope below 10 K in Fig. 4(b) corresponds to a value of 0.2 meV for E_{ba}. Using τ_{rb} = 3.3 μsec and assuming that a singlet level is far enough in this temperature range and that $P_a = 2P_b$, the relaxation rate obtained from the slow component indicates that a two-phonon process is dominant above 20 K; the result is shown in Fig. 6. The result on RbI[7] may be analyzed with the same idea shown here.

The parameters obtained thus far and the excitonic structure could be related with the 290 nm and 338 nm intrinsic exciton bands in

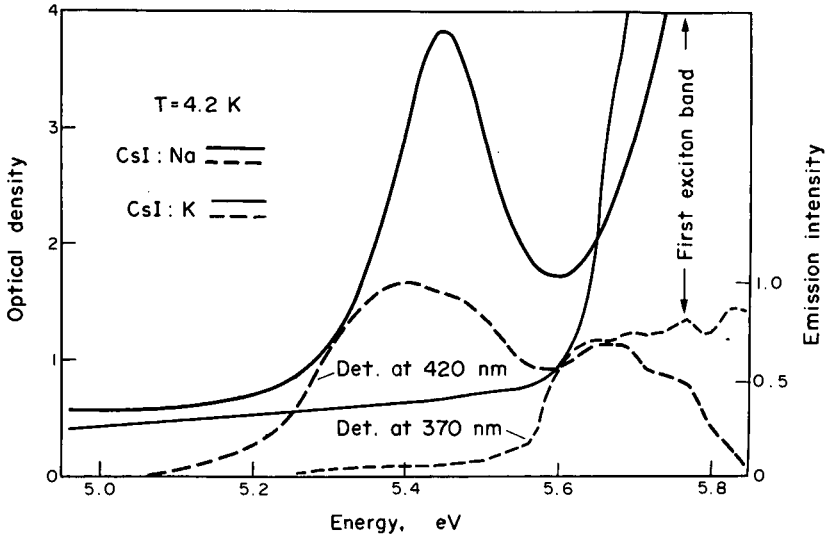

Fig. 3 The optical absorption (solid lines) and excitation spectra (dotted lines) of CsI:Na and CsI:K crystals. Thick lines and thin lines are for CsI:Na and CsI:K crystals respectively. The absorption is measured with 2.5 mm thick CsI:Na and 0.4 mm CsI:K crystals; the luminescence is detected at 420 nm and 370 nm, respectively.

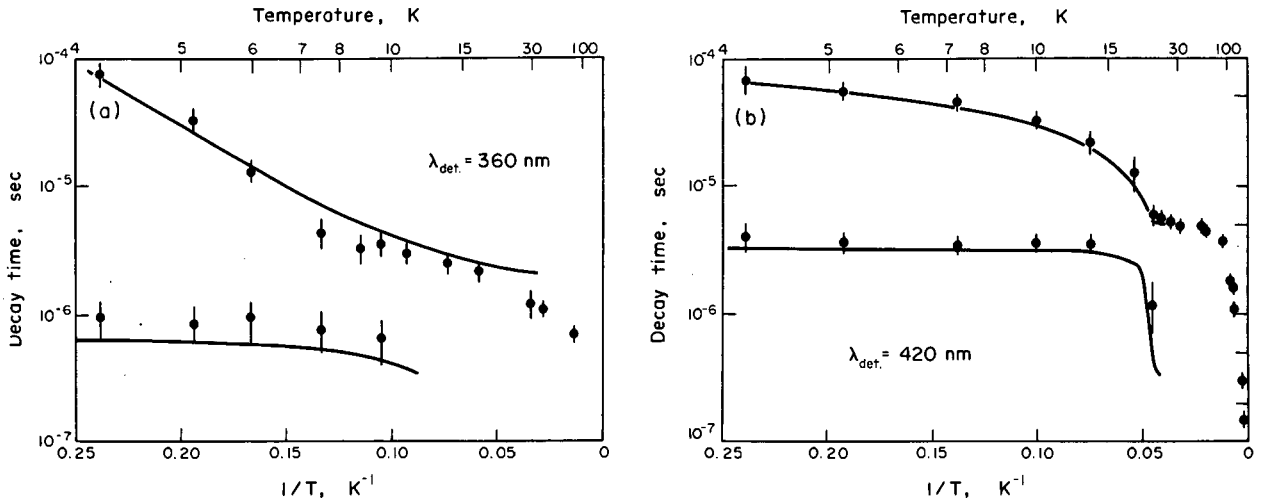

Fig. 4 (a) and (b)
Decay times of 370 (a) and 420 (b) bands as a function of temperature. The solid lines are obtained with the model of Fig. 5 with relaxation rates P_a and P_b determined by a one-phonon process for (a) and shown by solid line in Fig. 6 for (b).

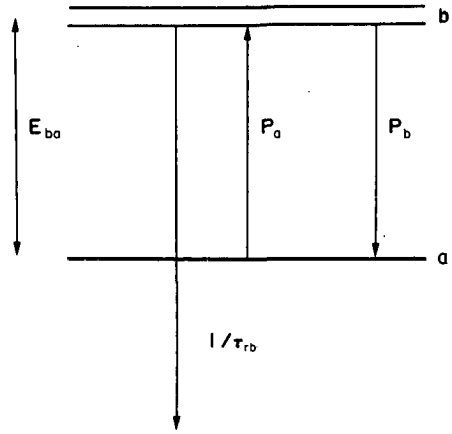

Fig. 5 Energy levels of the triplet exciton and transitions rates. The levels a and b correspond to A_u and E_u levels of the self-trapped exciton in the CsCl lattice[10]. $1/\tau_{rb}$ is the radiative transition rate to the ground state (Ag) and P_a and P_b are relaxation rates in the triplet state.

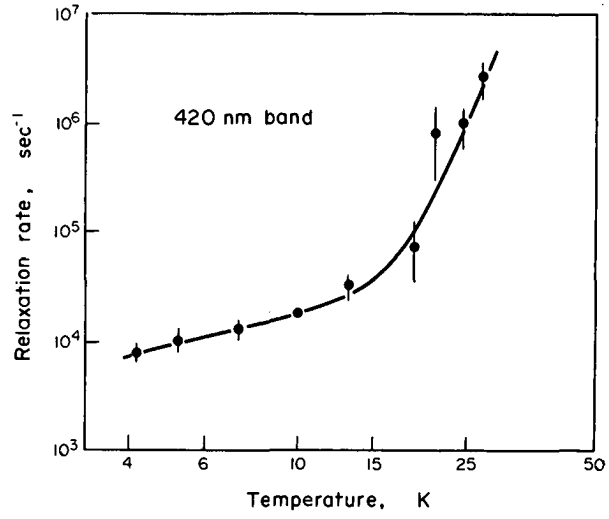

Fig. 6 The relaxation rate P_b of the triplet state VS temperature estimated from the slow component of the decay time of the 420 band shown in Fig. 4(a). The solid line is given by $P_b = 1.8\times10^3\ T + 2.5\times10^{-7}\ T^9$.

CsI[8]. Although the 420 band has singlet and triplet components and the 370 band has only a triplet component like the 290 and 338 bands[9] respectively, further precise studies such as magnetic circular polarization are necessary.

The decay time decreases further when the temperature increases above 70 and 30 K in the cases of 420 and 370 bands. Applying the equation $1/\tau(T) = 1/\tau(70\ K) + (1/\tau_o)\exp(-\Delta E/kT)$ based on a thermally activated non-radiative process for the 420 band above 70 K, one obtains $\tau_o = (4\pm2)\times10^{-8}$ sec, $\Delta E = 0.03\pm0.01$ eV. However, the luminescence intensity of the 420 band is nearly constant from 4.2 to 300 K under continuous UV excitation. This apparent discrepancy suggests the increase of the quantum yield to create the relaxed exciton at higher temperature. Furthermore, a time delay of about 100 nsec between the pulse excitation and the growth of the 420 band has been found at 300 K. Comprehension of these experimental results will be useful to understand the strong efficiency of the blue luminescence even at room temperature.

In conclusion, the basic mechanism of the 420 nm luminescence in CsI:Na at low temperature is bound to singlet and triplet excitons, the two-phonon relaxation process playing a decisive role in the temperature dependence of the decay time. The high efficiency of this luminescence at room temperature might be due to the creation process of the excitons.

Acknowledgment - The authors are indebted to Dr. V. Skarda for crystal growth and to the Swiss National Science Foundation for financial support.

REFERENCES

1 T. Sidler, J.P. Pellaux, A. Nouailhat and M.A. Aegerter; Journal of Phys. C9-34, 89 (1973).
2 A.N. Panova and N.V. Shiran; Bull. Acad. Sci. USSR, Phys. Ser. 31, 866 (1967), and Opt. Spektrosk. 32, 111 (1972).
3 O.L. Hsu and C.W. Bate; Journal of Lum. 15, 75 (1977).
4 J. Menefee, Y. Cho and C. Swinehart; IEEE Trans. Nucl. Sci. S-14, 1 (1967).
5 In the case of UV excitation, both 370 and 420 bands can occur in either CsI:Na or CsI:K crystals if the excitation wavelength is properly choosen. This is probably due to K^+ and Na^+ impurities in the initial powder (1×10^{-4} ppm in CsI).
6 The decay time of the 370 band has been measured in both crystals by assuming the same origin.
7 J.U. Fischbach, D. Fröhlich and M.N. Kabler; Journal of Lum. 6, 29 (1973).
8 H. Lamatsch, J. Rossel and E. Saurer; Phys. Stat. Sol. 41, 605 (1970).
9 J.P. Pellaux, T. Iida, J.P. von der Weid and M.A. Aegerter; Journal of Phys. C 13, 1009 (1980).
10 W.B. Fowler, M.J. Marrone, M.N. Kabler; Phys. Rev. B8, 5909 (1973).

Solid State Communications, Vol.42, No.3, pp.185-187, 1982. 0038-1098/82/150185-03$03.00/0
Printed in Great Britain. Pergamon Press Ltd.

TIME EVOLUTION OF TUNNELLING RECOMBINATION LUMINESCENCE IN CsI:Na

A.-H.Kayal, A.C.Mezger, J.Rossel , and K.Imanaka

Institut de Physique, Universite de Neuchâtel,
2000 NE, Switzerland

(received 10 November 1981 by G.F. Bassani)

The decay of the tunnelling recombination luminescence (TRL) of V_k and Na^o centers is studied by means of a pulsed optical stimulation of the Na^o band. The results are well interpreted by a model in which the TRL intensity is expressed by the sum of the successive luminescences from the self-trapped exciton (STE) perturbed by a Na^+ ion as the final emitting state of the TRL; the STE are formed successively depending on the distances between V_k and Na^o centers which are randomly distributed in the crystal.

An ionizing irradiation of CsI:Na cryatals at low temperatures produces stable V_k and Na^o (electron trapped on Na^+ ion) centers which are accompanied with optical absorption bands peaked at 410 nm and 720 nm, respectively [1]. After such an irradiation, a luminescence at 420 nm due to the tunnelling recombination of V_k and Na^o centers is observed for a long time as in the case of some silver doped alkali halides (V_k-Ag^o). The decay of this tunnelling recombination luminescence (TRL) is well described by the model proposed by Delbecq et al.[2], in which the TRL decays with t^{-1}, in a time region longer than 1 ms after putting off the irradiation [3]. However, this rather macroscopic model cannot explain the behaviour of the decay in a shorter time region. To inveatigate the decay in this region is one of the purposes of this note.

In the preceding paper [4], we proposed, on the basis of magneto-optical experiments, that the TRL in CsI:Na occurs via the self-trapped exciton (STE) state perturbed by a Na^+ ion [5]. The main purpose of the present work is to verify this proposition from a standpoint of decay time of the STE: If the final emitting state of the TRL is the STE state, the decay of TRL just after putting off the ionizing irradiation should be determined by the lifetime of the exciton.

The decay of TRL in such a short time period has been studied, usually, by means of pulsed ionizing beams, e.g. pulsed X-rays and pulsed electron beams [6]. Instead of such high energy sources, we used the optical stimulation of the electron trap (Na^o) band by laser pulses on X-irradiated crystals. By this stimulation, electrons are liberated from Na^o to the conduction band giving the similar situation as by the pulsed ionizing irradiation. Then some of the electrons recombine with V_k centers resulting in the intrinsic luminescences of 290 and 338 nm, and the rest of them is trapped again on Na^+ ions and starts to tunnel.

The experiments were made at temperatures between 4.2 and 77 K for several concentrations of V_k (and Na^o) centers; the concentrations were controlled by the duration of X-ray irradiation at T < 30 K. A pulsed dye laser with pulse-width of 10 ns at a low repetition rate (0.5 to 2 Hz) was used for the optical stimulation of Na^o centers. Then, the decay signal of the luminescence induced by each laser pulse was stored in an waveform recorder and sent to a signal averager; the detail of experimental setup is the same as in ref.7. We confirmed that, at such a low repetition rate, the luminescence intensity just before the next pulse was small enough and contributing a DC level to the detector. Much attention was paid to the problem of bleaching of the centers during the measurements; the intensity of the laser pulse was enough weakened. Therefore, our measurements were restricted up to 77 K, since at higher temperatures, the V_k centers are not any longer stable causing a rapid bleaching of the centers [1].

Typical examples of the results at 4.2 K for low and high concentrations of centers are shown by dots in Figs.1 and 2, respectively. The solid curve on each figure shows theoretically best fitted one and is described later. In the case of either high concentrations or higher temperatures, rather anomalous plateaus were observed as seen in Fig.2. Such plateaus have been also observed by Tashiro et al. in NaCl:Ag [6].

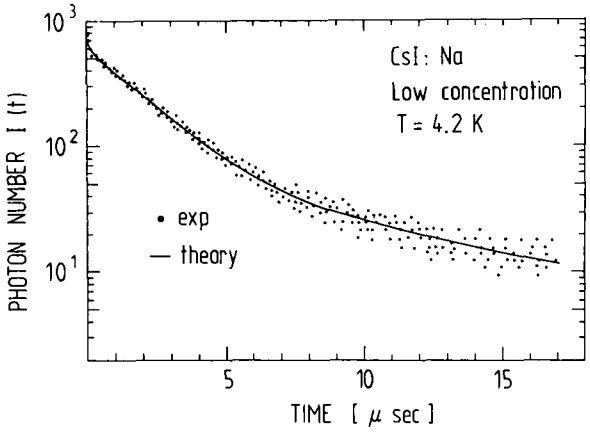

Fig.1. Decay of the TRL in CsI:Na at 4.2 K for low concentration of centers. Dots show a part of experimental results and solid curve is the theoretically best fitted curve.

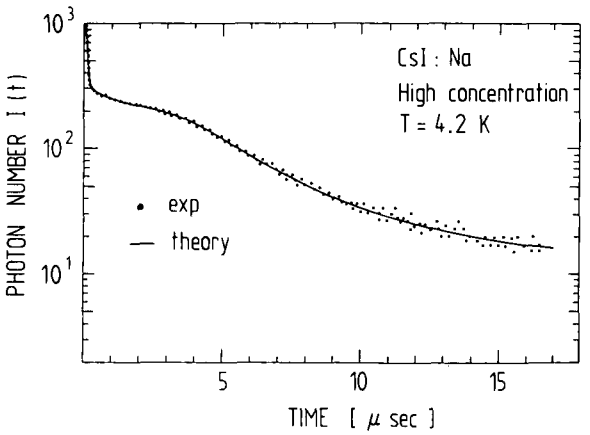

Fig.2 Decay of the TRL at 4.2 K for high concentration of centers.

In order to explain these experimental results, we express the decay of TRL, I(t), by the sum of STE's luminescences which start to occur after tunnelling time Δ of V_k to Na^o as

$$I(t)=N_o f(t)+\sum_{\Delta} N(\Delta) f(t-\Delta) \quad ,(\tau_o < \Delta < t) \qquad (1)$$

where τ_o is the fastest tunnelling time, N(Δ) the number of V_k-Na^o pairs which take the same tunnelling time Δ to recombine, and f(t) the waveform of the STE decay after recombination given by

$$f(t) = \sum_i A_i \exp\{-t/\tau_i\}, \qquad (2)$$

where τ_i's are the decay time-constants and A_i's the corresponding intensities. The first term in eq.(1) originates from the V_k-Na^o pairs which have already an appropriate distance at t=0 to form the STE without tunnelling or with a tunnelling time shorter than the laser pulse-width; N_o is the number of such pairs.

Just after the pulsed stimulation, the number of nearest neighbour V_k-Na^o pairs having the distance in the interval [r,r+dr] which will recombine by the tunnelling process is given by

$$N(r,dr) = 4\pi r^2 n \exp\{-4\pi r^3 n/3\}\, dr , \qquad (3)$$

where n denotes the number of centers per unit volume[8]. Furthermore, the tunnelling time Δ is related to the distance r as [9]

$$\Delta^{-1} = \tau_o^{-1} \exp\{-r/\lambda\} , \qquad (4)$$

where λ is a constant factor. By substituting r from eq.(4) into eq.(3), the number of pairs having the tunnelling time in the interval [Δ, Δ+dΔ], N(Δ,dΔ), is obtained. Then, the function N(Δ) appearing in eq.(1), which is proportional to N(Δ,dΔ), is expressed as follows;

$$N(\Delta) = C\Delta^{-1}[\ln(\Delta/\tau_o)]^2 \exp\{\Lambda[\ln\{\Delta/\tau_o)]^3\}, \qquad (5)$$

where $C=4\pi\lambda^3 n\gamma d\Delta$ and $\Lambda=4\pi\lambda^3 n/3$; γ represents the relative intensity of the second term to the first term in eq.(1). For the waveform of STE decay f(t) in eq.(2), we take three exponential decays as shown in Fig.3 resulting from the fact that the 420 nm band contains the emissions from the singlet and the triplet states [5]; τ_1 is the decay time of singlet state, τ_2 the direct decay of triplet, and τ_3 the indirect decay of triplet via multi-phonon processes. Then, by

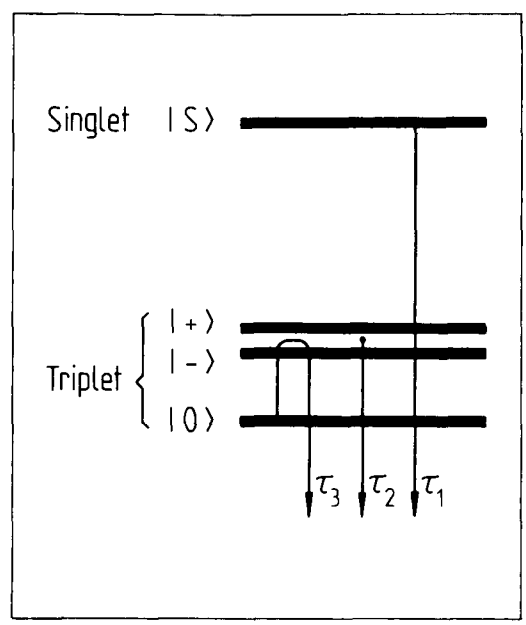

Fig.3. Energy scheme and decay rate of the STE in CsI:Na.

assuming a discrete tunnelling time Δ as $\Delta = \tau_o + (k-1)\delta$, i.e. the recombinations occur successively after each δ second, the second term in eq.(1) can be calculated by the summation over natural numbers k instead of Δ . This rather complicated procedure for the calculation of eq.(1) can be understood by Fig.4.

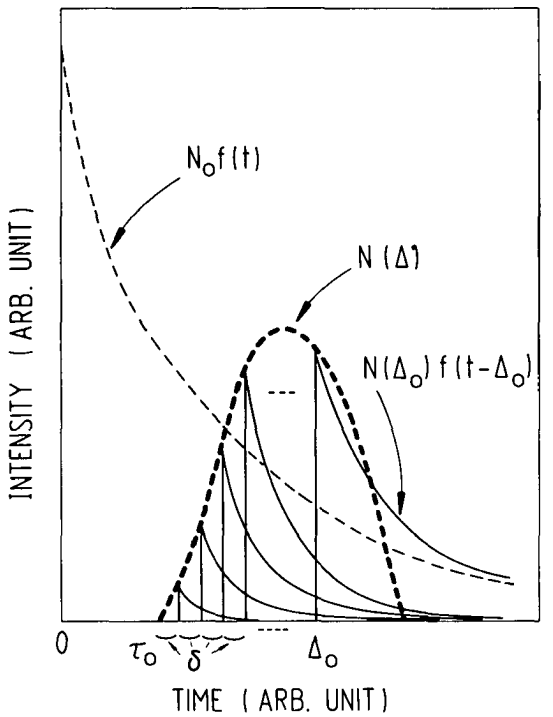

Fig.4. Schematic diagram of the calculation for the decay of TRL. The decay is given by adding the sum of $N(\Delta)f(t-\Delta)$'s to $N_o f(t)$. (See the text.)

Using this calculation, the experimental results are fitted to eq.(5) by adjusting the parameters with a least squares numerical method. In fact, however, the number of parameters is too high for a satisfactory analysis, so that the number of parameters is reduced in the following way. The value of τ_3 is directly determined by the experimental results observed in longer time scale (10 to 100 μs) which are not shown on the figures, A_1 is put to unity, and δ is fixed to 50 ns since this value is heavily correlated to that of C; if the magnitude of δ is decreased, the same value of I(t) can be obtained by decreasing C value, and vice versa.

Result of the computer curve-fitting gives good agreement for the decay times τ_1, τ_2, and τ_3 between different concentrationa of centers at the same temperature. Only the differences are in the values of τ_o, C, and Λ which are related to the concentrations. As an example, the theoretically best fitted curves shown by solid curves on Figs.1 and 2 are obtained by using the same values of the parameters τ_1, τ_2, and τ_3 which are 0.04, 2.3, and 60 μs, respectively, with different values for the parametera τ_o, C, and Λ which are 3.0 μs, 4.3×10^3, and 0.91 for Fig.1 and 0.28 μs, 8.5×10^3, and 0.08 for Fig.2, respectively. We are not able to deduce the physically meaningful quantities from the value of C and Λ since they contain an amplitude factor γ . However, the fastest tunnelling time τ_o being shorter in the case of higher concentration and the calculated peak positions of $N(\Delta)$ (6.4 μs for Fig.1 and 1.1 μs for Fig.2) seem to be reasonable. At temperatures higher than 20 K, only two components of decays are obtained; for example at 77 K, time constants are 0.25 and 5.3 μs.

These numerical values of the decay times agree quite well with those obtained in the case of STE luminescence by the UV light excitation [5] at temperatures from 4.2 to 77 K. Thus, our claim that the TRL occurs via the STE state perturbed by a Na^+ ion is justified.

In the present model, we could not succeed to explain the decay of TRL in the time region longer than 1 ms, where the Delbecq's t^{-1} law is valid, since calculated I(t) decays very rapidly after 1 ms. A consistent explanation which covers the complete time region requires further investigations.

Acknowledgements - The authors are indebted to the Swiss National Foundation for Scientific Research for the financial support of this work.

References

[1] T.Sidler, J.-P.Pellaux, A.Nouailhat, and M.A.Aegerter, Solid State Commun. 13, 479 (1973).

[2] C.J.Delbecq, Y.Toyozawa, and P.H.Yuster, Phys. Rev. B9, 4497 (1974).

[3] O.Thiébaud, J.-J.Pilloud, M.A.Aegerter, and C.Jaccard, J. de Physique C7, 169 (1976).

[4] K.Imanaka, A.-H.Kayal, A.C.Mezger, and J.Rossel, phys.stat.sol.(b)108, 449 (1981).

[5] A.-H.Kayal, Y.Mori, C.Jaccard, and J.Rossel, Solid State Commun. 35, 457 (1980).

[6] T.Tashiro, S.Takeuchi, M.Saidoh, and N.Itoh, phys. stat. sol. (b)92, 611 (1979).

[7] A.C.Mezger and C.Jaccard, phys.stat.sol. (b) 107, 689 (1981).

[8] S.Chandrasekhar, Rev.Mod.Phys.15, 86 (1943).

[9] D.L.Dexter, Phys. Rev. 93, 985 (1954).

Solid State Communications, Vol.34, pp.315-319.
Pergamon Press Ltd. 1980. Printed in Great Britain.

OPTICAL AND ESR STUDIES ON AN IR ABSORPTION BAND IN CsI:Na AFTER X-RAY IRRADIATION

Y. Mori*, A.H. Kayal and C. Jaccard

Institut de Physique, Université de Neuchâtel, Rue A.-L. Breguet 1,
CH - 2000 Neuchâtel (Switzerland)

and

M.A. Aegerter

Instituto de Fisica e Quimica de São Carlos, Universidade de São Paulo,
CEP 13560 São Carlos (Brazil)

(Received 20 February 1980 by F. Bassani)

We have studied the nature of the defect giving rise to a near IR absorption band (717 nm) in X irradiated CsI:Na by measuring its linear dichroism, its magnetic circular dichroism and its change due to the resonance microwave. The defect ($g_{||} = 1.96$, $g_{\perp} = 2.23$ with axis near <100>) involves a Na^+ ion and an excess electron.

1. INTRODUCTION

X-ray irradiation at low temperature usually creates in alkali halide crystals stable electron and hole centers at the same time, like F and V_k centers. This is not the case in pure CsI crystals, even below 4.2 K.

When CsI doped with NaI is irradiated at low temperature, two optical absorption bands appear at 408 and 717 nm[1]. The former one which is independent of doping impurities is attributed to the V_k center[2]. The latter near infrared absorption whose excitation leads to intrinsic recombination luminescence was supposed to be due to an electron trap such as Na^o [1].

ESR may be one of the best tools to study the origin of this absorption band as well as its atomic structure. However, ESR observed so far in CsI:Na with direct detection technique is only that of the V_k center[2]. In order to study the origin of this absorption, optical properties of this band including the magnetic circular dichroism (MCD) have been studied. We found ESR with X-band microwaves (9.1 GHz) by an optical detection technique in which the microwave induced change of MCD has been monitored.

2. EXPERIMENTAL

The optical absorption spectrum and its linear dichroism at 4.2 K together with the excitation spectrum for the 338 nm intrinsic recombination luminescence[3] around the absorption band are shown in Fig. 1. The total area of the IR absorption band is about 5 times as large as that of 408 nm band. The linear dichroism, the relative difference of absorption coefficients $\Delta\sigma = (\sigma_{||} - \sigma_{\perp})/(\sigma_{||} + \sigma_{\perp})$, has been measured after the bleaching with 660 nm and 770 nm light linearly polarized parallel to one of the <100> crystal axes. There is no dichroism apparently in both cases within 5% of experimental error. The excitation spectrum is very similar to the absorption spectrum. The excitation bleaches with equal rates both IR and V_k absorption bands.

The MCD spectra are shown in Fig. 2 for the case in which the magnetic field is applied parallel to <100> axis; similar results are obtained when the magnetic field is parallel to <111>. They are derivative type curves of the absorption band and they display the same shape over all the measured temperature and magnetic field region. The dependence of the MCD intensity at 680 nm on the temperature and the magnetic field are shown in Fig. 3. The result indicates that the MCD of this band is determined by the so-called paramagnetic term, that is, spin polarization in the ground state.

When the resonant microwave field H_1 is applied at 1.5 K to the crystal with a static magnetic field, the MCD decreases towards zero, since the microwave bleaches the ground state spin polarization; the MCD decreases up to about 20% of its initial value showing a characteristic saturation with increasing microwave power. Since the MCD is determined

*On leave from the Department of Applied Physics, Osaka City University, Osaka (Japan)

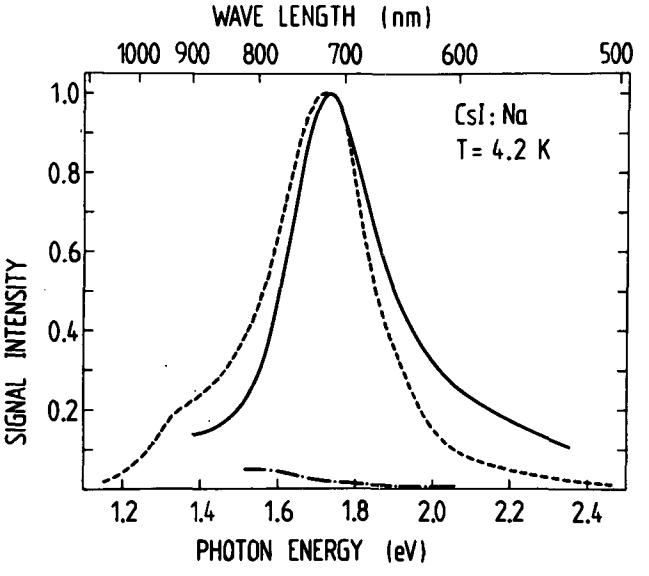

Fig. 1

Solid, dashed and dotted lines show optical absorption (in arbitrary unit), its linear dichroism $(\sigma_{//} - \sigma_{\perp})/(\sigma_{//} + \sigma_{\perp})$, and excitation spectrum (a.u) of the 338 nm intrinsic recombination luminescence at 4.2 K, respectively, after X-ray irradiation on CsI:Na crystal. Lower and higher energy sides of the absorption measurement are limited by the spectrometer and the glass filter used to cut the luminescence.

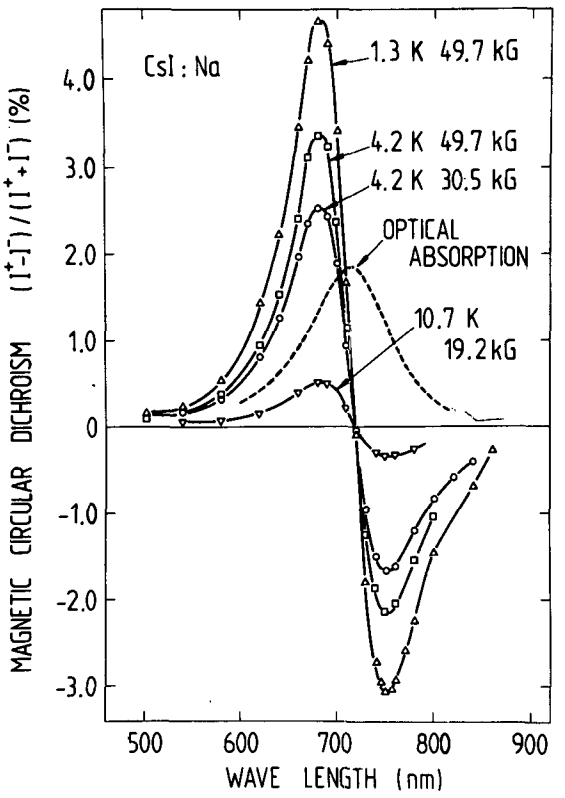

Fig. 2

Magnetic circular dichroism of the IR absorption band on Fig. 1 at several temperatures and magnetic fields.

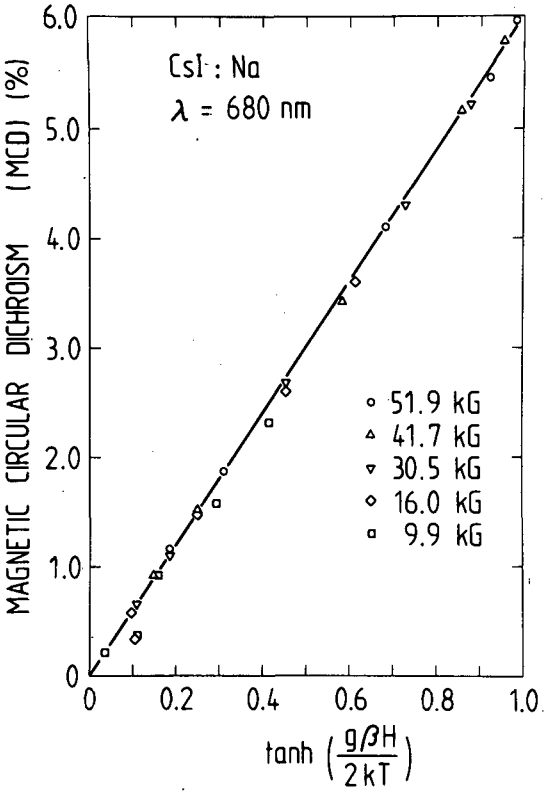

Fig. 3

The dependence of the magnetic circular dichroism intentity at 680 nm on the temperature and on the magnetic field which is applied parallel to <100>.

by spin polarization in these experimental conditions for ESR, one can obtain an ESR spectrum as $[MCD(H_1 = 0) - MCD(H_1)]/MCD(H_1 = 0)$ as shown in Fig. 4 (a), (b) when the magnetic field is applied parallel to the <100> and <111> directions, respectively; the MCD is monitored at 680 nm to give the spectra of Fig. 4.

When the magnetic field is applied parallel to the <111> direction, the overall features of the ESR spectrum are symmetric around the peak position. When the field is parallel to <100>, the ESR is asymmetric and shows another peak on the higher field side. The similar spectrum has been obtained at 4.2 K. These results, together with the spectrum obtained with the magnetic field parallel to <110>, show that the symmetry of the center is lower than O_h and that its symmetry axis is parallel or near to the <100> axis.

3. DISCUSSION

ESR spectra have been analyzed by means of the method of moments by assuming the symmetry axis parallel to the <100> axis and the axial symmetric spin Hamiltonian

$$\mathcal{H} = \beta[g_{\parallel} H_z S_z + g_{\perp}(H_x S_x + H_y S_y)] + \sum_i \vec{I}_i \cdot \tilde{A}_i \cdot \vec{S} \qquad (1)$$

where the last term is the hyperfine interaction with nuclei. Furthermore, we tentatively assume isotropic optical absorption coefficient, since there was no linear dichroism. One can obtain $g_{\parallel}$ and $g_{\perp}$ of 1.97 ± 0.02 and 2.23 ± 0.02, respectively, from the first moments of the ESR spectra under three configurations of the magnetic field. Peak positions according to these g-value are shown in Fig. 4 (a), (b) by solid arrows.

The following facts suggest that the center is associated with an electron; the center is created by X-ray together with the V_k center and the excitation of this IR band enhances the intrinsic recombination luminescence and bleaches the V_k and IR absorption bands. On the other hand, one may imagine an hole center from the rather large positive g-shift of $g_{\parallel}$. One should check the possibility that the IR absorption band is produced by the overlap of two absorption bands due to electron and hole

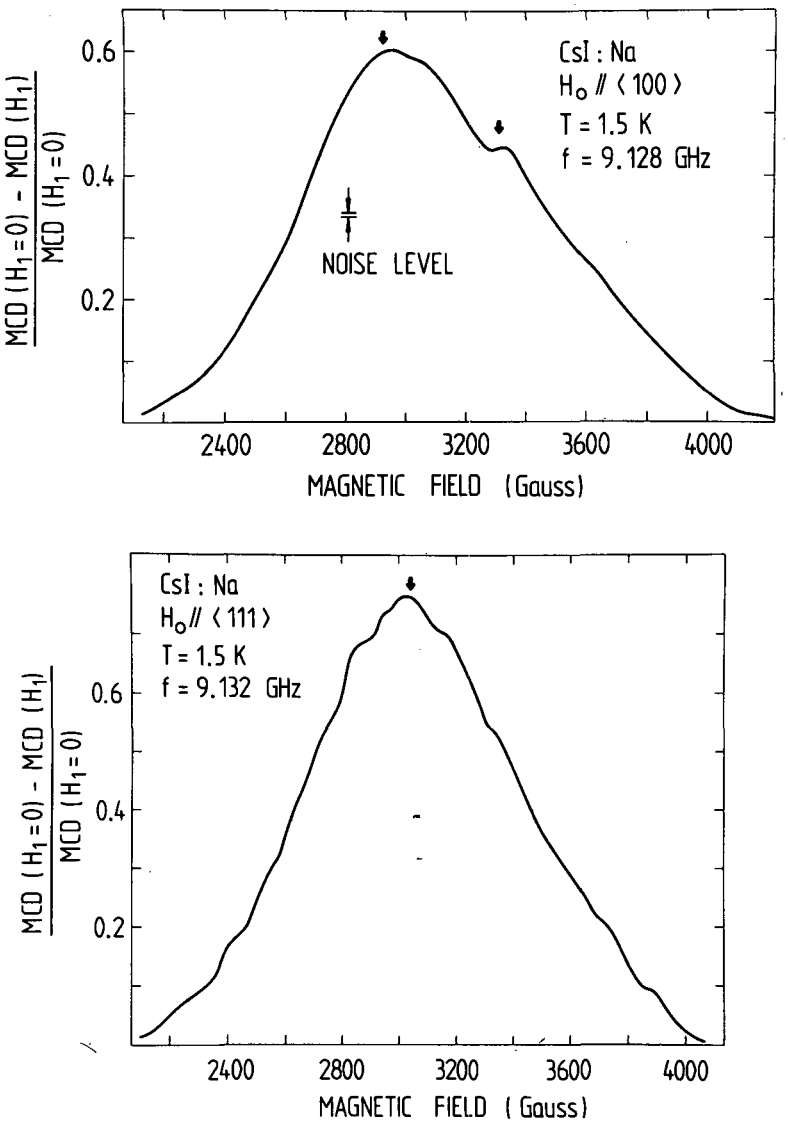

Fig. 4

ESR spectra (a) and (b) obtained by means of the optical detection technique at 1.5 K with the magnetic field parallel to <100> (f_0 = 9.128 GHz) and to <111> (9.132 GHz), respectively.

centers. The following facts suggest that the absorption band, or at least most of it, is due to one center only : (1) the excitation spectrum is very similar to the absorption band; (2) the MCD spectrum is independent of the magnetic field and of the temperature; (3) the ESR spectra obtained by monitoring MCD at 630 and 800 nm are the same as those at 680 nm; (4) the saturation recovery curves of the ESR signal are the same at several magnetic fields over the ESR spectrum.

If the center moves by changing the direction of its symmetry axis, the absence of linear dichroism does not indicate necessarily an isotropic absorption coefficient. It is possible to fit the first moments within experimental error by using the anisotropic absorption coefficients within the region of $|\Delta\sigma| < 0.4$; the set of g-values is the same as in the previous case. The second moment analysis has been tried with the spin Hamiltonian of eq. (1) and the assumption that the principal axes of the hf tensor are the same as those of the g-tensor. In this analysis, theoretical values can fit the experimental ones only when one introduces the anisotropy of the absorption coeffieicnet. Our assumptions such as isotropy of the absorption coefficient, and the possibility of minor contribution from another center, must be checked by more precise experiments. Furthermore, temperature dependence of ESR

including relaxation time would be interesting to see dynamical effects of this center.

4. CONCLUSION

A paramagnetic center associated with the Na^+ ion and an electron gives the IR absorption band peaked at 717 nm produced by X-ray in CsI:Na. The center has a symmetry lower than O_h, the principal axis lying around <100> and the g-values being $g_{\parallel} = 1.97 \pm 0.02$ and $g_{\perp} = 2.23 \pm 0.02$. This indicates that the paramagnetic spin is not simply due to a 3s electron on a Na^+ ion.

Acknowledgment - One of the authors (Y.M.) wishes to thank Dr. J.J. Pilloud for his discussions. We are grateful to the Swiss National Science Foundation and FINEP (Brazil) for financial support.

REFERENCES

1. T. SIDLER, J.P. PELLAUX, A. NOUAILHAT and M.A. AEGERTER, Journal de Physique, Colloque C9-89 (1973).

2. J.J. PILLOUD and C. JACCARD, Solid State Commun. 17, 907 (1975).

3. H. LAMATSCH, J. ROSSEL and E. SAURER, Phys. Stat. Sol. (b) 46, 687 (1971).

Solid State Communications, Vol.41, No.1, pp.69-74, 1982
Printed in Great Britain.

0038-1098/82/010069-06$02.00/0
Pergamon Press Ltd.

A SEARCH FOR Na ATOM IN CsI:Na CRYSTAL

Y. Mori*, A.-H. Kayal and C. Jaccard**

Institut de Physique, Université de Neuchâtel
CH-2000 Neuchâtel, Switzerland

(Received 20 September 1981 by F. Bassani)

The presence of a Na atom in CsI:Na after X-ray irradiation is searched by ESR (35 GHz microwave) detected through the magnetic circular dichroism of a related optical absorption band. The results are discussed with the model of Na atom in the crystal where either 3s or 3 p_z orbit is the ground state depending on its site.

1. Introduction

X irradiation of a CsI:Na crystal at low temperature creates the optical absorption band due to the V_k center, and another optical absorption band peaked at 717 nm which is supposed to be due to a localized excess electron center such as Na^o. [1,2]

In ref. 1, it was found that (a) the excitation of the band leads to the intrinsic recombination luminescence[3] with an excitation spectrum similar to the absorption, (b) the magnetic circular dichroism (MCD) of the band is determined by the paramagnetic term with a negative spin-orbit interaction constant λ and (c) ESR found by an optical detection technique with 9.1 GHz microwaves and its moment analysis, assuming a single origin of the ESR, show a symmetry of the related center lower than O_h and a positive g shift.

In the present work, several optical absorption bands associated with Na^+ ions have been found by measuring the absorption and the MCD at the lower energy tail of the band so far studied (called here IR band). The higher frequency microwaves (35 GHz) have been applied for ESR in order to improve the resolution and the precision; three types of ESR line were found. The MCD spectrum of the IR band has been decomposed into three bands by measuring the monitor wavelength dependence of ESR. The result indicates that the peaks of the three bands composing the IR band are all located around 720 nm.

2. Experimental

The samples cut with (100) faces were annealed at 450°C to eliminate internal strains. After X irradiation at liquid He temperature, the crystal was kept in liquid He during the run of the experiments.

The spectra shown in Fig. 1 are those for the optical absorption and for the excitation of the 338 nm intrinsic recombination luminescence; the absence of further absorption band was confirmed for photon energies down to 0.5 eV. The absorption and excitation spectra are quite similar to each other over all the measured wavelength region, including the shoulder at 900 nm. Beside the intrinsic recombination, the recombination luminescence peaked at 420 nm[4] was also enhanced by the IR band excitation, but it is much weaker.

As already confirmed in ref. 1, the MCD monitored at 680 nm is determined by spin pola-

---

Present address

* Department of Applied Physics, Osaka City University, Sugimoto-cho, Osaka, Japan 558

** Swiss Federal Institute for Snow and Avalanche Research, 7260 Weissfluhjoch/Davos, Switzerland

*

Another idea to explain the large positive g-shift for an excess electron was proposed by Prof. R.H. Bartram (Physics Department, University of Connecticut, USA). The basic idea is charge transfer from I_2^{--} to Na^o after trapping of an electron. In the final state, the Na^- is no more paramagnetic while I_2^- is like the V_k center. The authors are indebted to him for the proposal.

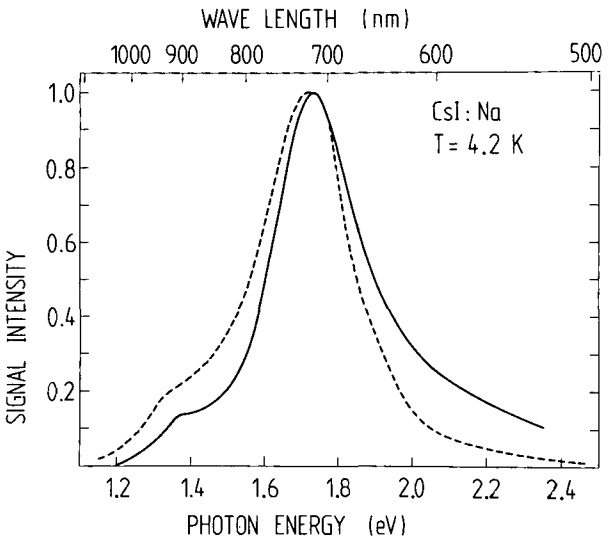

Fig. 1 : Spectra of the optical absorption (solid line), the IR band, and the excitation (dotted line) for the 338 nm intrinsic recombination luminescence at 4.2 K, respectively, after X irradiation of CsI:Na crystals.

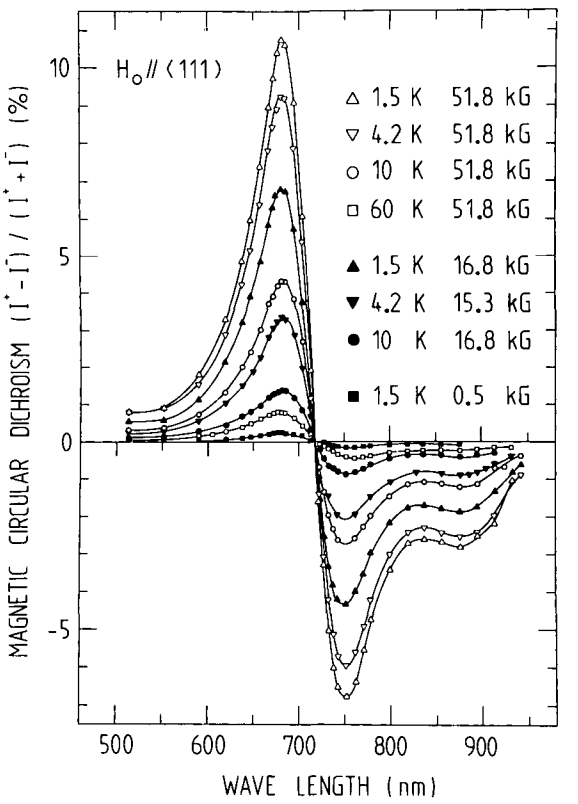

Fig. 2 : Magnetic circular dichroism of the IR absorption band of Fig. 1 at several temperatures and magnetic fields which are applied parallel to <111> direction.

rization of the ground state. Furthermore the MCD line shape, which has a derivative type curve around the main peak as shown in Fig. 2, is independent of the measured temperature T (1.5 to 60 K) and magnetic field H_0 (0.5 to 50 kG). From these two facts, we conclude that the MCD of the whole IR absorption band, which extends from 400 nm to 1000 nm, is determined by the ground state spin polarization. On the basis of this conclusion, we measured the ESR of centers related to the IR band at several wavelengths by means of Q-band (35 GHz) microwaves; the same technique and processes as in ref. 1 were used.

The ESR spectra shown in Fig. 3(a), (b) and (c) are those obtained at 900 nm under magnetic field applied parallel to the <100>, <110> and <111> directions, respectively. The angular dependence can be understood, if we assume that the center has a 4-fold symmetry around the axis parallel to the <100> direction, and that the ESR of the center whose axis is parallel to the magnetic field is not observed because of a selection rule of the optical absorption in the related band. The second assumption means that a σ-type dipole transition is the dominant optical absorption of the center, or $\alpha_{\parallel} \gg \alpha_{\perp}$ in the optical absorption constant. With these assumptions, we can determine a set of parameters which are shown in Table 1.

When we measured the MCD at 675 nm, ESR spectra observed are different from those shown in Fig. 3. This is demonstrated in Fig. 4(a), (b) and (c); the ESR line detected at 11.4 kG in the case of Fig. 3(a) is quite small in Fig. 4 (a). In all these figures, one can see a part of a Gaussian-like smooth curve peaked at g = 1.89 (13.4 kG in Fig. 4(a)). Based on this fact, we decomposed these spectra into two curves which are symmetric around each peak. The analysis of the Gaussian-like line results in isotropic parameters as shown in Table 1, while the analysis of the angular dependence of the other one by means of a spin Hamiltonian for $S = \frac{1}{2}$ with axial symmetry, was not successful. Further discussion of the latter will be given later.

In order to know the relative contribution of these centers to the IR band, the dependence of ESR on the wavelength of the MCD monitor beam was measured in the case of a magnetic field parallel to <111> direction. Those spectra were decomposed into three ESR lines so far observed as shown in Figs. 3(c) and 4(c). The MCD spectrum has been decomposed into three lines by assuming the same value of proportionality constants between MCD and ESR intensities for three lines. The result shown in Fig. 5 suggests that the IR band is composed of three absorption bands whose peak energy E_{abs} are all located around 1.7 eV where we can see the peak of the IR band; widths ΔE_{MCD}^{P-P} of these bands are listed in Table 1.

3. Discussion

The excitation of IR band at any wavelength, (a) produces the intrinsic recombination luminescence peaked at either 338 nm or 290 nm depending on temperature, (b) bleaches the IR band and (c) at the same time, bleaches the absorption band due to the V_k center peaked

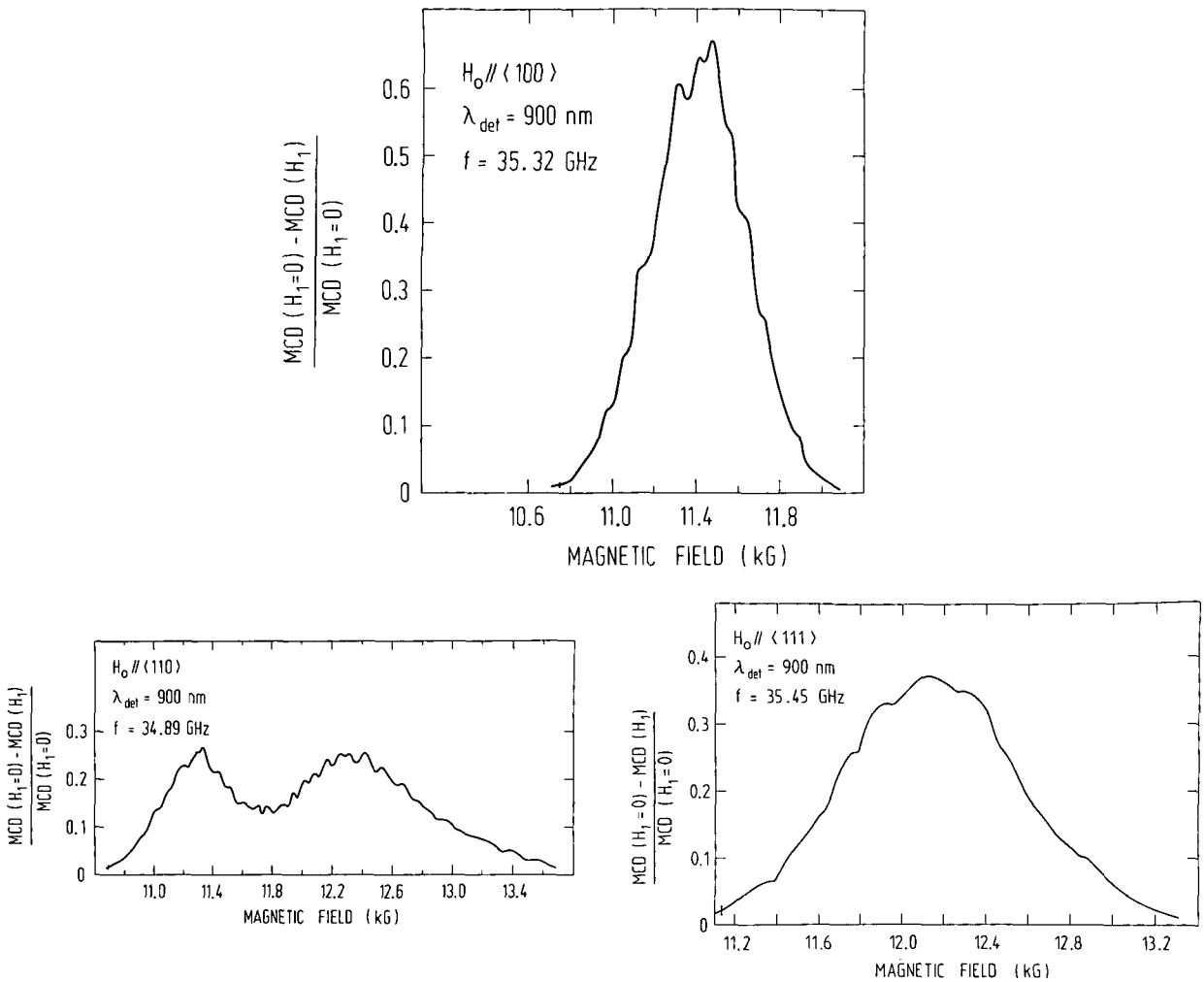

Fig. 3 : ESR spectra (a), (b) and (c) obtained by means of the optical detection technique at 1.5 K with the magnetic field parallel to the <100>, <110> and <111> directions, respectively. The MCD was monitored at the wavelength of 900 nm.

at 410 nm.[1] These experimental facts strongly suggest that the excitation of the IR band creates a free electron in the conduction band, yielding the intrinsic recombination luminescence even at 1.5 K. Thus, the IR band would be due to an excess electron forming a center associated with a Na^+ ion; final states of the optical absorption band are in the conduction band. The minor effect that the excitation yields also the recombination luminescence perturbed by Na ions (420 nm band) could be interpreted as follows : a free electron created by the IR band excitation is trapped at another Na^+ ion which is sufficiently near to the V_k center so as to recombine with it through the tunneling process.[5]

Being supported by the idea described above, we propose the following tentative model drawn in Fig. 6, describing the centers A and C of the Table 1. According to this model, a substitutional Na atom which traps an excess electron has two stable positions, depending on the orbits of the excess electron. The Na atom can be on a lattice site, then the electron can be trapped on the 3s orbit. On the other hand, when the electron is trapped on the 3 p_z orbit, the Na atom is located at a stable position displaced in the <100> direction from the lattice site. Therefore the optical absorption can be due to an electric dipole transition from 3s to 3p states in the former case, while it can be from $3p_z$ to $3d_{x^2-y^2}$ in the latter case. The presence of two positive ions on the [001] axis in the second shell is important in a situation such as shown in Fig. 6 and with transition energy of 1.7 eV for both cases, since the extension of the $3p_z$ orbit on these two ions can play an important role to lower the energy; notice that the energy difference from 3s to 3p and from 3p to 3d are 2.11 and 1.51 eV, respec-

Table 1 : Properties of three optical absorption bands, and ESR lines related with the IR absorption band in CsI:Na. Values for the F center and the Na free atom are also tabulated for comparison.

TABLE 1

Parameters / Centers	E_{abs} (eV)	ΔE^{P-P}_{MCD} (eV)	E_f (eV)	α_{abs}	λ (meV)	g	σ (G)
A	1.7	0.16	positive	isotropic	negative	1.89	325
B	1.7	0.22	positive	$\alpha_{\parallel} \leq \alpha_{\perp}$	negative	~ 2	
C	1.7	0.62	positive	$\alpha_{\parallel} \gg \alpha_{\perp}$	negative	$g_{\parallel} = 1.82$ $g_{\perp} = 2.21$	$\sigma_{\parallel} = 240$ $\sigma_{\perp} = 640$
F	1.68	0.1	-0.052	isotropic	-40	1.9	365
Na^o	$E_{3s-3p}=2.21$ $E_{3p-3d}=1.51$		-		1.4		352

tively, in the case of a free atom.

As shown in Table 1, the center A exhibits similar properties as those of the F center, except for the energy E_f of the final state of the absorption, which is higher than the bottom of the conduction band. This similarity can be reasonably explained by the fact that the F center is well approximated as an alkali atom in the crystal. The larger energy of E_f compared with the F center can be due to the fact that an electron trapped by Na^+ ion is a local extra charge. As for the total hf interaction strength σ (second moment) of the Na atom and the F center, the main difference lies in the presence of a central nucleus, in the case of the Na atom. Thus the ground state wavefunction must be a diffused one to give a value of the hf interaction strength similar to that of the F center as shown in Table 1. This diffused wavefunction is consistent with the higher energy E_f.

The center C has axial symmetry (D_{4h} or C_{4v}) with the axis parallel to the <100> direction. The characteristic points of this center, compared with centers A or F, are its symmetry, a large positive g-shift in $g_{\perp}$ in spite of an excess electron center and a very large band width in optical absorption. According to the model proposed above, these characteristics can be explained as follows. The mechanism of the positive g-shift is due to the large spin-orbit interaction constants of I^- and Cs^+ ions which contribute through the orthogonalization of the excess electron wavefunction with the ion cores. In other words, a negative spin-orbit interaction constant leads to a positive g-shift.[6] Such a negative spin-orbit interaction constant occurs in the unrelaxed excited state of the F center[7] or in our experimental results of MCD for the center A and C shown in Fig. 2 *. The ground state of the center C is very near to the bottom of the conduction band, so that the absorption band has a very large width as in the case of the F' center.[8]

The center B has a more complicated nature than A or C. Its ESR spectra shown in Fig. 4 are not isotropic. However, they display apparently a single line in each magnetic field direction. This results either from a partial loss of the ESR lines due to the selection rule of the optical transition as in the case of the center C, or from a very small anisotropy of the g-values in the center B. Another difficulty for the analysis of those results is the consistent understanding of ESR spectra obtained with 9.1 GHz and 35 GHz microwaves. One cannot reproduce

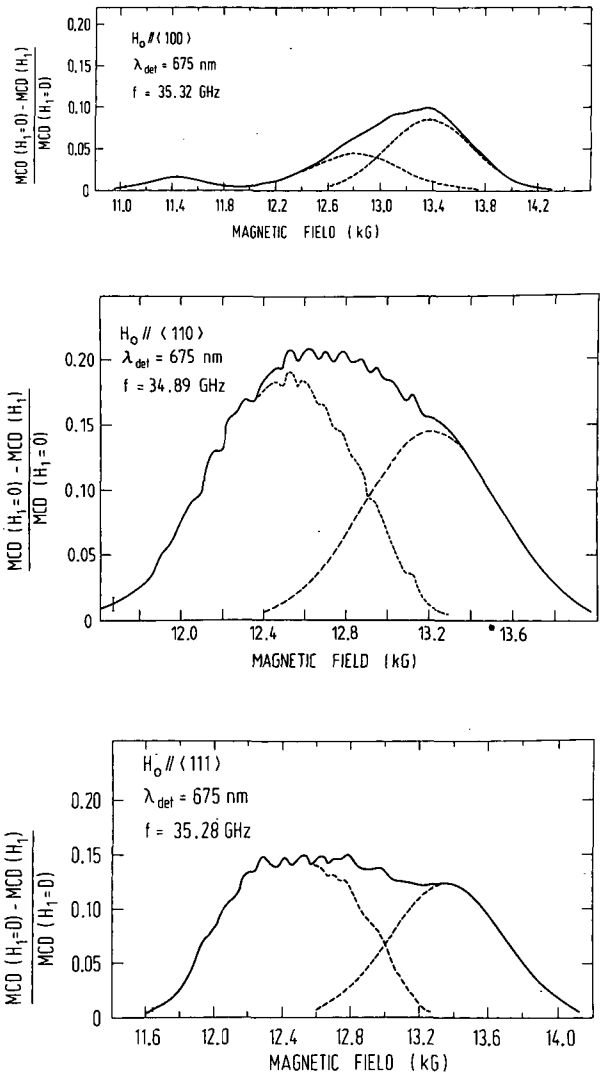

Fig. 4 : ESR spectra (a), (b) and (c) obtained by means of the optical detection technique at 1.5 K with the magnetic field parallel to the <100>, <110> and <111> directions, respectively. The MCD was monitored at the wavelength of 675 nm.

the ESR spectrum obtained with 9.1 GHz microwaves by starting from the ESR line with 35 GHz microwaves without taking into account the magnetic field dependence of processes to detect the ESR, especially when the magnetic field is applied parallel to the <100> direction. Known characteristics of the center B are listed in Table 1.

We have observed three different states of the localized electron. So, if those three states are due to centers which are composed of different atomic elements, each center could give different recombination luminescence associated with a Na^+ ion. However, only one strong recombination luminescence band, that is the 420 nm band, has been observed in CsI:Na so far with X-ray excitation. The centers A and C

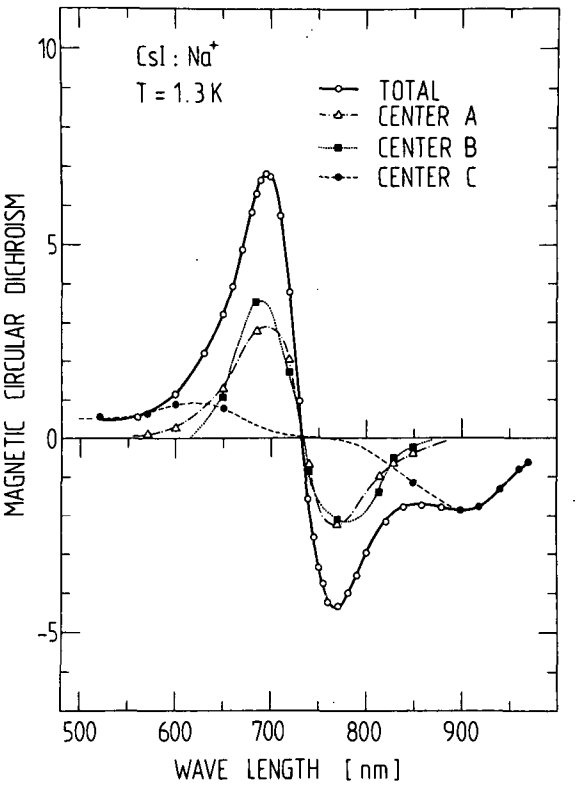

Fig. 5 : Decomposition of the magnetic circular dichroism into three contributions which have been found in ESR shown in Figs. 3 and 4. The MCD is decomposed into three lines according to a relative ESR intensity at each monitor wavelength; the ESR was measured with the magnetic field parallel to <111>.

could result in the same exciton after the lattice relaxation during the formation process. Furthermore, the diffused localized electron can be a trap for a hole migrating in the crystal. This might partly explain why the efficiency of the 420 nm band is so high even at room temperature.

The existence of stable electron trap in CsI doped with Li^+, K^+, Rb^+ ions has been checked after the X irradiation at low temperature. The presence of the V_k absorption band or of absorption bands in the visible or near infrared region down to 900 nm has not been observed. This implies that the mechanism of electron trapping in CsI crystal is not simply due to the difference of ionization energy in these ions. The lattice relaxation plays certainly an important role in producing a strong electron trap in CsI:Na crystals.

4. Conclusion

X irradiation of CsI:Na crystal at low temperatures creates paramagnetic centers associated with Na ions in three types of states of excess electron. The centers which have symmetries of O_h, lower than O_h with 4-fold axis parallel to <100> axis, and lower than O_h, res-

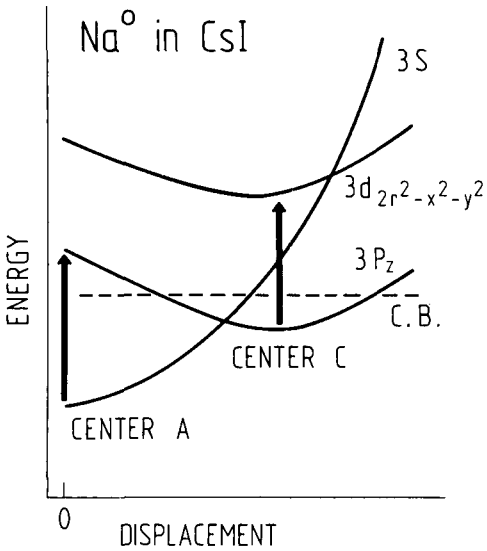

Fig. 6 : Model for the optical absorption of a Na atom in CsI crystal. Stable sites of the atom depend on orbits on which an excess electron has been trapped. Final states of the optical absorption bands must be in the conduction band. The displacement is meant along the <100> direction from a lattice site.

pectively, give optical absorption bands peaked all around 720 nm. A tentative model has been proposed for the first two centers by assuming a Na atom in the crystal.

Acknowledgement - The authors wish to thank Dr. K. Imanaka for his discussions. This work has been supported by the Swiss National Science Foundation.

References

1. Y. Mori, A.H. Kayal, C. Jaccard and M.A. Aegerter, Solid State Comm. 34, 315 (1980).
2. C.K. Ong, K.S. Song, R. Monnier and A.M. Stoneham, J. Phys. C 12, 4641 (1979).
3. T. Iida, Y. Nakaoka, J.P. von der Weid and M.A. Aegerter, J. Phys. C 13, 983 (1980).
4. A.H. Kayal, Y. Mori, C. Jaccard and J. Rossel, Solid State Comm. 35, 457 (1980).
5. K. Imanaka, A.H. Kayal, A. Mezger and J. Rossel, (submitted to Phys. Stat. Solidi (b)).
6. A.M. Stoneham, Theory of Defects in Solids, p. 448. Clarendon Press, Oxford (1975).
7. C.H. Henry and C.P. Slichter, Physics of Color Centers, chapter 6. Academic Press, N.Y. (1968), ed. W.B. Fowler.
8. W.B. Fowler, Physics of Color Centers, chapter 2. Academic Press, N.Y. (1968), ed. W.B. Fowler.

PUBLICATIONS

1. Luminescence processes in CsI doped with Na^+ and K^+ ions, Solid State Comm. 35, 457 (1980).

2. Optical and ESR studies on an IR absorption band in CsI:Na after X-ray irradiation, Solid State Comm. 34, 315 (1980).

3. Self-trapped exciton luminescence after tunnelling of V_K and Na^0 centers in CsI:Na crystals, Physica Status Solidi (b), 108, 449 (1981).

4. Excitons perturbed by sodium ion in CsI:Na crystal, Physica Status Solidi (b) 110, 115 (1982).

5. A search for Na atom in CsI:Na crystal, Solid State Comm. 41, 69 (1982).

6. Time evolution of tunnelling recombination luminescence in CsI:Na, Solid State Comm. 42, 185 (1982).

VERSIONS INTEGRALES DE LA THESE DEPOSEES A

- La Bibliothèque de l'Institut de Physique de l'Université de Neuchâtel

- La Bibliothèque de l'Université de Neuchâtel.